

progression and for providing an anti-apoptotic survival activity necessary for Ras-induced transformation<sup>13</sup>. These Rac-dependent growth-promoting signals are likely to be the outcome of superoxide production through a mechanism that is similar to the Rac2-promoted activation of the NADPH oxidase system in phagocytes. It has also been shown that malignant transformation mediated by a constitutively active Cdc42 mutant Cdc42(F28L) is eliminated when the insert helix is deleted from the activated Cdc42 molecule<sup>14</sup>. Cdc42 does not stimulate NADPH oxidase activity nor is it thought to cause superoxide production and, at the present time, the identity of the effector responsible for mediating the insert-dependent transforming signal of Cdc42 has not been identified. A provocative possibility is that this cell growth-promoting effect of Cdc42 is related to the recent finding that Cdc42 stimulation of phospholipase D activity requires the insert helix<sup>15</sup>. Phospholipase D1 (PLD1) generates phosphatidic acid, a known mitogenic precursor, and Cdc42 was shown to bind PLD1 in a GTP-dependent man-

ner. Removal of the Cdc42 insert helix did not interfere with binding to PLD1 but completely eliminated stimulation of PLD activity.

By analogy with the interaction between Rac2 and cyt b described above, it is attractive to consider a model where the switch I domain of Cdc42 mediates GTP-dependent binding to PLD1, while the insert region makes contacts with the enzyme that contribute directly to the catalysis of lipid hydrolysis. The analogy might even be carried one step further, given that both the Arf GTP-binding protein and protein kinase C (PKC) are capable of independently stimulating PLD1 activity. These proteins act synergistically with Cdc42 and other Rho proteins to further stimulate PLD1 activity. It is tempting to imagine that the combined effects of Cdc42, Arf and PKC on PLD1 may occur through a similar mechanism as the combined regulatory effects of Rac and p67<sup>phox</sup> on cyt b. Thus, the work of Diebold and Bokoch gives us much to think about in terms of the mechanisms by which small GTP-binding proteins may regulate diverse cellular activities that extend

beyond the role of the phagocyte in the immune response.

1. Babior, B. M. *Blood* 93, 1464–1476 (1999).
2. Abo, A., Boyhan, A., West, L., Thrasher, A. J. & Segal, A. W. *J. Biol. Chem.* 267, 16767–16770 (1992).
3. Diebold, B. A. & Bokoch, G. M. *Nature Immunol.* 2, 211–215 (2001).
4. Nisimoto, Y., Freeman, I. L. R., Motalebi, S. A., Hirshberg, M. & Lambeth, I. D. *J. Biol. Chem.* 272, 18834–18841 (1997).
5. Freeman, I. L. R., Abo, A. & Lambeth, I. D. *J. Biol. Chem.* 271, 19794–19801 (1996).
6. Henderson, L. M. & Chappell, J. B. *Biochim. Biophys. Acta* 1273, 87–107 (1996).
7. Lapouge, K. et al. *Mol. Cell.* 6, 899–907 (2000).
8. Ahmed, S. et al. *J. Biol. Chem.* 273, 15693–15701 (1998).
9. Han, C., Freeman, I. L. R., Lee, T., Motalebi, S. A. & Lambeth, I. D. *J. Biol. Chem.* 273, 16663–16668 (1998).
10. Hoffman, G. R., Nassar, N. & Cerione, R. A. *Cell* 100, 345–356 (2000).
11. Morreale, A. et al. *Nature Struct. Biol.* 7, 384–388 (2000).
12. Goldberg, I. *Cell* 96, 893–902 (1999).
13. Joneson, T. & Bar-Sagi, D. *A. J. Biol. Chem.* 273, 17991–17994 (1998).
14. Wu, W. J., Lin, R., Cerione, R. A. & Manor, D. *J. Biol. Chem.* 273, 16655–16658 (1998).
15. Walker, S. L., Wu, W., Cerione, R. A. & Brown, H. A. *J. Biol. Chem.* 275, 15665–15668 (2000).

Departments of <sup>1</sup>Chemistry and Chemical Biology and <sup>2</sup>Molecular Medicine, Cornell University, Ithaca, NY 14853, USA. (rac1@cornell.edu)

## Les liaisons dangereuses

BERNARD MALISSEN



A minimal half-life of the TCR-pMHC interaction is required for complete T cell signaling (the kinetic proof reading model). In an extension to this model it is clear that the dwell time or half-life of TCR-pMHC interaction is also critical for T cell activation

Resting T cells circulate continuously throughout the peripheral lymphoid organs where they scan the surface of antigen-presenting cells (APCs) for the presence of foreign peptide fragments bound in the groove of major histocompatibility complex (MHC) molecules. Detection of a specific peptide-MHC (pMHC) complex, expressed on APCs at a density of 0.1–1 molecules/μm<sup>2</sup>, is sufficient to trigger robust T cell activation. To carry out this formidable task, T cells use a specific receptor—the T cell antigen receptor (TCR)—that recognizes a specific pMHC complex and relays the information to the interior of the T cell (Fig. 1a). Most receptors encountered in biology are precommitted to bind a given ligand with invariant parameters. In contrast, the antigen-binding site of the TCR is formed by stochastic somatic DNA recombinations and can interact with different affinities with a spectrum of peptides complexed to a self-MHC molecule. Importantly, the TCR appears to be capable of translating small quantitative differences in ligand binding into qualitatively different signals.

In turn, this leads to T cell responses that range from maximal activation to desensitization. The ability to produce such a diverse range of responses plays a role in thymic selection and may have an impact on interclonal competition during the course of an immune response. In this issue of *Nature Immunology*, a report by Nathenson and colleagues provides a link between the kinetics of TCR-pMHC interactions and the effectiveness of T cell responses<sup>1</sup>. Distinct mutations affecting residues important for antigen recognition by the TCR led to either shortened or prolonged TCR-pMHC interactions. Interestingly, both types of mutations were found to be detrimental for T cell activation.

Any ligand-receptor interaction that occurs in solution and displays a simple reversible 1:1 binding can be described by the rate of spontaneous association ( $k_{on}$ ) and dissociation ( $k_{off}$ ), and by their ratio  $k_{off}/k_{on}$ , known as the dissociation constant ( $K_D$ ). The ability to engineer soluble monomeric TCR and pMHC molecules led to the characterization of the kinetic and thermodynamic parameters of a few TCR-pMHC interactions<sup>2,3</sup>. Low-affinity values ( $K_D=1–90$  μM at 25 °C) reported for agonistic pMHC ligands resulted from both slow  $k_{on}$  and fast  $k_{off}$  values. The unusually slow  $k_{on}$  noted for TCR-pMHC interactions is probably due to structural readjustments that occur in the TCR complementarity determining regions (CDRs) upon binding to the pMHC surface<sup>4</sup>. A given TCR can bind to a self-MHC molecule complexed to the cognate peptide or to some of its structural analogs obtained by mutating the peptide residues that correspond to TCR-contact sites. The distinct half-lives ( $t_{1/2}$ , and note that  $k_{off} = \ln 2/t_{1/2}$ ) of these interactions constitutes a better predictor of the biological potency of ligands than the  $K_D$  value<sup>5</sup>.

In the case of the 2B4 TCR, half-lives of approximately 12, 2, and 0.2 s were determined for pMHC complexes that behaved as a strong agonist, as a weak agonist (capable of eliciting only a portion of the activating events) or as an antagonist (capable of weakening or preventing activation by agonists), respectively. This rather



of the corresponding TCR-pMHC interactions. Given the variety of assays used to estimate the parameters of TCR-pMHC interactions, it is difficult to make comparisons among different studies. It is, however, possible to incorporate all these data within the frame of a Gaussian half-life-effect curve, as long as it is assumed that the A6 TCR-HTLV-1 Tax peptide-HLA-A2<sup>7</sup> and the 2C TCR-dEV8-H-2K<sup>b</sup> (ref. 8) complexes ranked fortuitously at its upper and lower end, respectively. A few other cases exist where the  $k_{\text{off}}$  of the TCR-pMHC interaction is not the sole determinant of biological activity<sup>9</sup>. Related to this, it should be mentioned that some of the TCR mutants engineered by Kalergis and colleagues show an increase in binding, but not in apparent half-life, which pointed towards an effect of some CDR3 $\beta$  mutation on the  $k_{\text{on}}$  value. The  $k_{\text{on}}$  of sets of related receptor-ligand combinations, where induced-fit mechanisms do not occur, are generally similar to each other. In addition, their respective  $K_D$  values for a fixed

ligand usually correlate with their  $k_{\text{off}}$  values (a measure of the number and the quality of all atomic interactions within the receptor-ligand binding interface). However, considering that both the length and the composition of CDR3s vary from one TCR to another and probably control the breadth of binding-site flexibility, it is likely that extensive analysis of TCR-pMHC interactions will reveal that  $k_{\text{on}}$  values are not confined to a narrow range and a more rapid  $k_{\text{on}}$  may also improve serial triggering.

Contrasting with the view that it is the  $k_{\text{off}}$ , rather than the  $K_D$ , that determines pMHC bioactivity, for some cytotoxic effector T cells it has been shown that a decrease in the  $k_{\text{off}}$  of the TCR-pMHC interaction could be compensated for by increasing the pMHC density on target cells<sup>10</sup>. This may reflect the fact that the molecular interactions occurring between two apposed cell membranes cannot be studied simply by using parameters extracted from conventional methods dealing with soluble reagents<sup>11</sup>. Regardless of the

above limitations, the recent possibility to manufacture *in vitro* TCR with an affinity 100-fold higher than that of naturally occurring ones<sup>12</sup>, should provide very appropriate reagents to further assess the effects of TCR-pMHC affinity on T cell responses.

1. Kalergis, A. M. et al. *Nature Immunol.* **2**, 229–234 (2001).
2. Willcox, B. E. et al. *Immunity* **10**, 357–365 (1999).
3. Boniface, J. J., Reich, Z., Lyons, D. S. & Davis, M. M. *Proc. Natl Acad. Sci. USA* **96**, 11446–11451 (1999).
4. Hennecke, J. & Wiley, D. C. *Cell* **104**, 1–4 (2001).
5. Grakoui, A. et al. *Science* **285**, 221–227 (1999).
6. Valitutti, S., Müller, S., Cella, M., Padovan, E. & Lanzavecchia, A. *Nature* **375**, 148–151 (1995).
7. Degano, M. et al. *Immunity* **12**, 251–261 (2000).
8. Baker, B. M., Gagnon, S. J., Biddison, W. E. & Wiley, D. C. *Immunity* **13**, 475–484 (2000).
9. Alam, S. M. et al. *Immunity* **10**, 227–237 (1999).
10. Bachmann, M. F., Salzmann, M., Oxenius, A. & Ohashi, P. S. *Eur. J. Immunol.* **28**, 2571–2579 (1998).
11. Van der Merwe, P. A. *Curr. Biol.* **9**, 419–422 (1999).
12. Holler, P. D. et al. *Proc. Natl Acad. Sci. USA* **97**, 5387–5392 (2000).

Centre d'Immunologie de Marseille-Luminy, INSERM-CNRS-Univ. Med., Case 906, 13288 Marseille Cedex 9, France. (bernardm@ciml.univ-mrs.fr)

## Multifaceted roles of MHC class I and MHC class I-like molecules in T cell activation

SOPHIE UGOLINI<sup>1</sup> AND ERIC VIVIER<sup>2</sup>

The  $\alpha\beta$  T lymphocytes recognize antigens presented in the groove of classical major histocompatibility (MHC) molecules via their T cell receptor (TCR). This paradigm is central to our understanding of the immune response. However, it has recently been recognized that classical MHC class I (MHC class Ia) and MHC class I-like molecules interact with many other receptors whose engagement controls T cell activation. In this issue of *Nature Immunology*, Spies and colleagues provide new information concerning this phenomenon. They show that NKG2D, a receptor for the MHC class I-like molecules called MIC, can serve as a costimulatory molecule on cytomegalovirus (CMV)-specific CD28-CD8<sup>+</sup> T cells<sup>1</sup>. These data are important for two reasons. First, they reveal an unexpected role for MIC molecules during viral infection. Second, they reveal a role for NKG2D as a costimulatory molecule for  $\alpha\beta$  TCR signals and thus contribute to the “chiseling out” of a new paradigm in the field of T cell activation.

MHC class I chain-related proteins called

MICA and MICB are human MHC class I-like molecules that do not bind either peptides or peptide surrogates (such as lipids) and do not associate with  $\beta_2$ -microglobulin<sup>2</sup>. The expression of MIC molecules has been reported in the intestinal epithelium as well as in diverse tumors of epithelial origin<sup>3</sup>. Spies and colleagues show that CMV infection induces MIC expression on *in vitro*-infected fibroblasts and endothelial cells<sup>1</sup>. In addition, they report the expression of MIC proteins in lung tissue sections from CMV-infected patients. These data extend the spectrum of MIC distribution and indicate that the cell surface expression of MIC protein can be up-regulated not only by heat shock but also upon CMV infection. Whether other viral infections and cellular distress factors provide the signals necessary to induce MIC cell-surface expression is an open question, one which will be undoubtedly investigated in the near future.

MIC molecules interact with NKG2D<sup>4</sup>. Human NKG2D is a lectin molecule that is expressed on the vast majority (if not all) of  $\gamma\delta$  T

In addition to the TCR and classical MHC class I, MHC class I-like molecules can interact with a variety of receptors that play a role in T cell activation. Engagement of NKG2D on CMV-specific  $\alpha\beta$  CD8<sup>+</sup> cells by MIC was found to provide them with a costimulatory signal and augment their cytotoxic response.

cells, CD8<sup>+</sup> T cells and natural killer (NK) cells as well as on a small subset of CD4<sup>+</sup> T cells<sup>5</sup>. In addition, mouse NKG2D has been described on activated macrophages<sup>6</sup>. MHC class I-like ligands for NKG2D, other than MIC molecules, have also recently been identified. They include UL-16 binding proteins (ULBP) in humans<sup>7</sup>, as well as retinoic acid early transcript 1 (Rae-1) and H-60 (a previously described minor histocompatibility antigen) in the mouse<sup>8,9</sup>. Soluble human NKG2D lectin domains can also bind soluble purified HLA-A, HLA-B and HLA-C molecules on their own<sup>8</sup>, although no cellular assays have completed this study. Spies and colleagues now show that MIC-NKG2D engagement on human CD8<sup>+</sup>CD28<sup>+</sup>  $\alpha\beta$  T cells augments their cytotoxic response and provides them with a costimulatory signal for cytokine production and proliferation<sup>1</sup>. Although the formal demonstration that NKG2D-signals are dependent upon  $\alpha\beta$  TCR engagement is not included in the article by Groh *et al.*, the new data strongly suggest that NKG2D engagement



# Breaking the affinity ceiling for antibodies and T cell receptors

Jefferson Foote<sup>\*†</sup> and Herman N. Eisen<sup>\*‡</sup>

<sup>\*</sup>Program in Molecular Medicine, Fred Hutchinson Cancer Research Center, Seattle, WA 98109; <sup>†</sup>Department of Immunology, University of Washington, Seattle, WA 98195; and <sup>‡</sup>Center for Cancer Research and Department of Biology, Massachusetts Institute of Technology, Cambridge, MA 02139

The antigen receptors made by lymphocytes are antibodies, which exist as soluble and cell-bound molecules, and T cell receptors (TCRs), which are always found on cell surfaces. The function of these receptors in immunity depends on their specificity and affinity for antigen. Specificity—the potential to bind one unique chemical structure more strongly than a number of similar alternatives—is established by antibody and TCR gene rearrangements early in a lymphocyte's ontogeny. Affinity—the equilibrium constant for antigen complexation (which we express as a dissociation constant,  $K_d$ )—can increase radically in the antibody-producing B lymphocytes as a result of somatic hypermutation of antibody genes and selection of cells with improved binding phenotype (1, 2), an antigen-driven process known as affinity maturation. Although the extent of somatic hypermutation of rearranged TCR genes remains controversial (3), affinity maturation of T lymphocytes at the level of cell populations by selection of the available repertoire recently has been described (4).

The affinities of antibodies and TCR obtained *in vivo* tend to fall within characteristic ranges constrained by biological requirements imposed during the ontogeny of B and T cells, about which more will be said later. Affinity maturation *in vitro*, as a rule, is not subject to the same biological constraints. In particular, affinity ceilings observed *in vivo* should not apply. The affinities of exhaustively *in vitro* matured antibodies or TCR should instead approach either a methodological ceiling intrinsic to the specific maturation protocol used or a molecular ceiling intrinsic to the architecture of antibodies and TCR. Two papers in PNAS describe *in vitro* affinity maturation of a TCR and an antibody using an ingenious system of yeast surface display (5, 6). *In vitro* TCR affinity maturation has not been reported previously. *In vitro* affinity maturation of antibodies has been described by several groups (7, 8), but never with so spectacular an endpoint, a  $K_d$  of  $5 \times 10^{-14}$  M. In both the TCR and antibody cases the

affinities ultimately obtained are orders of magnitude beyond the affinity ceilings observed *in vivo*. In this commentary we compare the *in vivo* affinity constraints with the *in vitro* constraints of the yeast system and comment on how breaking the affinity ceiling may affect basic immunology and immunotherapy.

## Yeast Display

Boder and Wittrup (9) several years ago developed a yeast-based system for surface display of recombinant proteins. The main element of this system is a fusion of the recombinant gene to the AGA2 gene of *Saccharomyces cerevisiae*. The AGA2 fusion protein is secreted and attaches through two disulfide bonds to the AGA1 gene product, which is covalently linked to the fibrillar layer of the yeast cell wall (10). This arrangement leaves the recombinant fusion protein on the outside of the cell, hence biochemically selectable, and the gene encoding the fusion protein on a plasmid inside the same cell, hence recoverable. The yeast can display thousands of copies of the recombinant fusion protein per cell and can be stained with fluorescent ligands and sorted by flow cytometry.

## Antibodies

Besides recognizing antigen through their surface antibodies, B cells can internalize and fragment protein antigens and present antigen to T cells in the form of peptides bound in the groove of MHC molecules. Specific antigen recognition by a surface antibody on a B cell, followed by endocytosis, leads to efficient antigen presentation (11), initiating cytokine release, B and T cell proliferation and differentiation, somatic hypermutation, and so on. We argued in an earlier commentary (12) that the residence time of an antigen complexed to a B cell surface antibody would constrain the dissociation rate constant ( $k_{off}$ ) selectable *in vivo*. The kernel of our proposal was that antibody-antigen complexes with lifetimes much longer than the time necessary for uptake would all be processed equally well, hence could not be distinguished. Batista and Neuberger

(13) recently demonstrated that this is so. They cocultured antilysozyme antibody transfectomas with lysozyme-specific T cell hybridomas, added soluble lysozyme at various concentrations, and monitored IL-2 release by the hybridomas as an indicator of antigen presentation. The lifetime of the antibody-lysozyme complex was varied by mutations in either the lysozyme or antibody. The result was that antibody-lysozyme pairs with a bound lifetime of 12 min or less showed an IL-2-vs.-antigen response that was very sensitive to  $k_{off}$ , whereas all pairs with a longer lifetime behaved identically regardless of  $k_{off}$ .

Residence time of an antigen bound to a surface antibody is also a key parameter in the *in vitro* affinity maturation system, although the antigen is not internalized by the yeast cells. In this method, yeast expressing a library of mutant antibodies are first saturated with fluorescent antigen, then treated with a nonfluorescent competitor antigen. Excess competitor makes dissociation of the fluorescent antigen effectively irreversible, and gradually the labeled cells lose their fluorescence. The time the competition is allowed to continue is critical. If too short, fluorescence differences between the wild type and a slower-dissociating mutant will be indistinct. If too long, all cells will be equally nonfluorescent. Boder and Wittrup (14) developed an elegant mathematical foundation for an optimal selection strategy. Given some typical experimental conditions and a desire for moderate stepwise improvements in  $k_{off}$ , the optimal incubation time for a selection step is approximately  $5/k_{off}$ . Boder *et al.* (6) used this model assiduously in the antibody *in vitro* affinity maturation work. They made kinetic measurements at each of four rounds of mutagenesis and selection of an anti-fluorescein antibody and adjusted compe-

See companion articles on page 5387 in issue 10 of volume 97 and on page 10701 of this issue.

<sup>‡</sup>To whom reprint requests should be addressed at: Center for Cancer Research, E17-128, Massachusetts Institute of Technology, 40 Ames Street, Cambridge, MA 02139-4307. E-mail: heisen@MIT.edu.

titution times and flow sorting parameters accordingly. Their results beautifully match the theory, and antibody-hapten stabilities of selected mutants march in clusters down a  $k_{\text{off}}$  plot, with regular kinetic improvements at each round of mutagenesis and selection. In the final round, incubation of labeled cells with nonfluorescent competitor continued for 5 days, a far longer interval than the 12-min window observed *in vivo* (13). Remarkably, the improvements in  $k_{\text{off}}$  and in affinity showed no sign of reaching a plateau in the last round. Therefore, neither an intrinsic molecular ceiling for antibody-hapten affinity nor a methodological ceiling inherent in the mutagenesis and selection protocol was reached. However, the methodological ceiling must be near: a further round of affinity maturation would require incubation with competitor to last on the order of a month. During this time the yeast would have to remain viable without dividing, and the surface antibody would have to resist unfolding.

### TCRs

The TCRs we discuss here are the  $\alpha\beta$  heterodimers present on most T cells. The natural ligands for these receptors are peptide-MHC (pMHC) complexes on the surface of other cells with which they are in contact. The peptides normally are derived by intracellular fragmentation of proteins, including indigenous or pathogen-encoded protein, but the MHC molecules are encoded by the host genome. Antigen recognition by T cells can result in various protective functions, including (i) destruction of virus-infected cells by cytolytic T lymphocytes that express the CD8 coreceptor, and (ii) release by various T cells expressing the CD4 coreceptor, of cytokines that either enhance antibody production by B cells or cause local inflammation.

Before discussing limits on TCR affinity *in vivo*, we note that evaluation of TCR-pMHC affinity and its significance is beset with methodological and conceptual problems. For one, the value of a TCR-pMHC affinity constant depends on the way the measurement is made. TCR affinity values generally are determined with monomeric soluble pMHC complexes either with the TCR having also been obtained in soluble form and immobilized on a biosensor chip ("cell-free" affinity), or with the TCR in its natural state as an integral membrane protein on live T cells. With live T cells,  $K_d$  values (intrinsic affinity) have been found to vary from slightly above 100  $\mu\text{M}$  to 0.1  $\mu\text{M}$ . In cell-free systems the values tend to be weaker. One difference is the absence in the cell-free system of the CD8 coreceptor found on cytotoxic T lymphocytes. CD8

interacts with a conserved MHC domain on target cells at a  $K_d$  of  $10^{-4}$  M, and the free energy of this interaction could boost the observed affinity of TCR for pMHC (15, 16). Second, specific T cell responses to the pMHC they recognize (also termed epitopes) on target cells appear to be determined by affinity of the TCR for its epitope and the number of copies of the epitope per target cell (epitope density). The epitope density is a fundamental parameter for interpreting TCR affinity as it applies to T cell function, yet epitope densities are difficult to measure and only a few values have been directly determined. The least ambiguous approximations come from cell lines expressing surface MHC molecules having empty peptide-binding sites. Extracellular peptides can bind to these MHC molecules, thereby creating epitopes on target cells. For peptides that react similarly with any particular MHC, relative epitope density values thus have been estimated from the concentration of free peptide needed to elicit a T cell response of a particular magnitude (e.g., half-maximal lysis of target cells in cytolytic reactions).

A TCR epitope includes both the antigenic peptide and adjacent regions of the MHC molecule's peptide-binding site. In developing the capacity for this dual recognition, T cell precursors in the thymus (thymocytes) undergo two processes that bear on the affinity ceiling for antigen recognition. T cell precursors able to recognize thymic (self) peptides bound to MHC are positively selected, in that they continue to develop. Perhaps 95% of cells fail this test and are eliminated, but the remainder are imprinted with an ability to recognize one or another of the host's own MHC molecules (17, 18). Negative selection in the thymus eliminates positively selected cells that react too strongly with thymic pMHC and thus could become dangerously autoreactive. The positive-negative selection model defines a window in which thymocytes die if TCR engagement by self-pMHC exceeds some upper affinity limit and fail to survive if below some lower limit (19). The actual limits have not been quantified. The affinity cutoff for negative selection in the thymus is the first of three *in vivo* TCR affinity ceilings we discuss.

The second affinity ceiling applies to mature T cells in encounters with antigen and is the intrinsic affinity sufficient for recognition of a vanishingly low epitope density, approaching 1 epitope per target cell. When TCR affinity is at the upper limit of the values determined on live cells ( $K_d$  0.1  $\mu\text{M}$ ), low epitope densities can elicit a strong T cell response with free peptide concentrations between 1 and 0.1 pM and fewer than 10 epitopes per target cell. Many orders of magnitude higher

free peptide concentrations are required to elicit similar responses when the TCR affinity is low, e.g., 100  $\mu\text{M}$ . As with B cells, T cells must engage antigen to survive, proliferate, and differentiate into memory cells. T cells able to respond to low epitope density will have a survival advantage over T cells that remain unreactive until high epitope density is reached. The reciprocal relation between epitope density and TCR affinity has an endpoint at  $<10$  pMHC molecules per target cell and TCR intrinsic  $K_d$   $10^{-7}$  M (20, 21). At this endpoint so few epitopes per target cell are required that the efficacy of T cells in cytolytic reactions would not be enhanced by higher intrinsic affinity values (20).

A third *in vivo* TCR affinity ceiling is possible (22). A passive limit for TCR affinity might be envisioned, in which, say,  $10^{-7}$  M is the maximum selectable affinity. Higher affinity clones arise, but with no reason for these clones to dominate the repertoire, are not detected. Alternatively, very high affinity—the result, say, of a very slow  $k_{\text{off}}$ —might be a disadvantage, and such T cells may fail to proliferate or even be actively eliminated, entailing a third affinity ceiling. Valitutti *et al.* (22) found that one pMHC on a B cell can engage and down-regulate many TCR on a T cell hybridoma. The serial engagement of TCR molecules on a T cell by pMHC on a target cell seems to be necessary for specific T cell responses, suggesting that transient signaling by many receptors gives a greater stimulus to cellular activation than constant signaling by a single receptor. If so, a clear rationale for an off-rate limit would be that an inability for pMHC to disengage from one TCR and rebind another would render a T cell less able to activate than one with a better balance between  $k_{\text{off}}$  and  $k_{\text{on}}$ .

In another type of recognition model, kinetic proofreading (23, 24), TCR-pMHC engagement is coupled to an exergonic specificity-validating process. This means of increasing biological specificity originally was formulated around the fidelity of protein synthesis, in which amino acid side chains of similar chemical structure must be distinguished (25). Such a model is attractive for T cell antigen recognition because the interaction of TCR with self-MHC and accessory molecules such as CD8 contribute to affinity without contributing to specificity, and the actual free energy of binding caused purely by the antigen is low. Kinetic proofreading is much more efficient if recognition of a cognate structure is not only enhanced, but inappropriate recognition of a noncognate structure is penalized (26). Models reformulated for T cell antigen recognition that embody this princi-



ple (25) can account for many observed phenomena, including antagonism of recognition by altered peptides. Such models typically equate long TCR-pepMHC complex lifetime with valid recognition and short lifetime with invalid recognition, respectively, yielding positive and negative signals for T cell activation. The import for a third affinity ceiling is that the optimal  $k_{\text{off}}$  is slow enough to guarantee sufficient time for the specificity validation process to initiate a positive signaling cascade. Still slower values are not an advantage, but neither are they a disadvantage unless a serial engagement mechanism operates as well.

Some recent studies contend that it is not the affinity of TCR-pepMHC interactions but the dissociation rate of the TCR-pepMHC complexes formed by this interaction that determine the T cell's response. The signal transduction reactions triggered by TCR ligation are unlikely to approach equilibrium, and the outcome of any particular reaction is indeed likely to depend on the stability of intermediate complexes. But TCR ligation by pepMHC, the initial step in T cell activation, has been shown to approach equilibrium (27), and thus the average number of TCR-pepMHC complexes formed in a T cell-target cell encounter is determined by the equilibrium constant. It is this number, together with the first-order dissociation of these complexes, that determines how many complexes survive long enough to trigger the next step in T cell activation. Thus it is not a question whether T cell responses are driven by  $k_{\text{off}}$  or affinity: both are linked in the initial TCR ligation reaction upon which specific T cell responses depend.

Holler *et al.* (5) derived a high-affinity TCR using yeast surface display methods

analogous to those described above for *in vitro* antibody maturation. Starting with a temperature-stabilized single-chain TCR from the receptor of an extensively studied T cell clone called 2C, they selected from a library of  $10^5$  yeast clones 15 mutants having higher affinity for a particular pepMHC complex. The affinity of the most reactive mutant (9 nM) was about 100 times greater than that of the original receptor.

### Concluding Remarks

The overall lesson from antibody and TCR *in vitro* affinity maturation is that mechanisms generating these molecules *in vivo* operate in an affinity regime far below the inherent potential of antibodies and TCR for ligand binding. The most significant aspect of *in vitro* affinity maturation of antibodies is perhaps practical, in that escape from the *in vivo* affinity ceiling may make possible an improved set of reagents for diagnosis and therapy. Breaking the TCR affinity ceiling has great practical ramifications as well, but equally significant are the possibilities created for testing fundamental hypotheses of T cell antigen recognition. The potential usefulness of high-affinity TCR is evident from the ability of the affinity matured 2C to specifically stain cells that display the appropriate pepMHC complexes. High-affinity TCR thus might provide specific reagents for measuring epitope densities. If they can be expressed on T cells, they also make it possible to determine an affinity limit above which T cell responses are impaired. They also could serve as useful reagents to detect particular pepMHC complexes important for stimulating the autoreactive T cells involved in autoimmune disorders.

A soluble molecule consisting of a TCR-like recognition component and a toxic effector component could be useful therapeutically for certain autoimmune or infectious or neoplastic diseases. The weak affinity of the currently available TCR has been a barrier to development of such fusion proteins for therapy. Their 0.1  $\mu\text{M}$  ceiling is in the range of only the weakest antibody affinity acceptable for therapy (28). The work by Holler *et al.* (5) clearly removes this barrier. However, another barrier arises from MHC polymorphism. A TCR specific for a particular epitope in one patient may be ineffective in others lacking that MHC, either because their MHC molecules do not bind the peptide or the resulting pepMHC complexes are not recognized by that TCR. And a third barrier may exist if a soluble high-affinity TCR were to react strongly with foreign (allogeneic) MHC—the phenomenon called alloreactivity. Nevertheless, under circumstances where a particular MHC molecule occurs frequently and its associated pathogenic peptide is known (e.g., HLA-DR4 and an encephalitogenic peptide in multiple sclerosis), a high-affinity TCR derived from a representative patient's T cells conceivably could prove useful in ablating undesirable antigen-presenting cells in many other affected individuals. Overall, high-affinity TCR generated by yeast display could provide the starting point for the development of novel diagnostic and therapeutic agents.

This research was supported by the Arthritis Foundation and National Science Foundation Grant 9807.950 (J.F.) and National Institute of Health Grants AI44477 and CA 60686 (H.N.E.).

1. Eisen, H. N. & Siskind, G. W. (1964) *Biochemistry* 3, 996–1008.
2. Rajewsky, K. (1996) *Nature (London)* 381, 751–758.
3. Zheng, B., Xue, W. & Kelsoe, G. (1994) *Nature (London)* 372, 556–559.
4. Busch, D. H. & Pamer, E. G. (1999) *J. Exp. Med.* 189, 701–710.
5. Holler, P. D., Holman, P. O., Shusta, E. V., O'Herrin, S., Wittrup, K. D. & Kranz, D. M. (2000) *Proc. Natl. Acad. Sci. USA* 97, 5387–5392.
6. Boder, E. T., Midelfort, K. S. & Wittrup, K. D. (2000) *Proc. Natl. Acad. Sci. USA* 97, 10701–10705.
7. Hawkins, R. E., Russell, S. J. & Winter, G. (1992) *J. Mol. Biol.* 226, 889–896.
8. Gram, H., Marconi, L. A., Barbas, C. F. D., Collet, T. A., Lerner, R. A. & Kang, A. S. (1992) *Proc. Natl. Acad. Sci. USA* 89, 3576–3580.
9. Boder, E. T. & Wittrup, K. D. (1997) *Nat. Biotechnol.* 15, 553–557.
10. Cappellaro, C., Baldermann, C., Rachel, R. &

- Tanner, W. (1994) *EMBO J.* 13, 4737–4744.
11. Lanzavecchia, A. (1985) *Nature (London)* 314, 537–539.
12. Foote, J. & Eisen, H. N. (1995) *Proc. Natl. Acad. Sci. USA* 92, 1054–1056.
13. Batista, F. D. & Neuberger, M. S. (1998) *Immunity* 8, 751–759.
14. Boder, E. T. & Wittrup, K. D. (1998) *Biotechnol. Prog.* 14, 55–62.
15. Garcia, K. C., Scott, C. A., Brunmark, A., Carbone, F. R., Peterson, P. A., Wilson, I. A. & Teyton, L. (1996) *Nature (London)* 384, 577–581.
16. Wyer, J. R., Willcox, B. E., Gao, G. F., Gerth, U. C., Davis, S. J., Bell, J. I., van der Merwe, P. A. & Jakobsen, B. K. (1999) *Immunity* 10, 219–225.
17. Shortman, K. & Scollay, R. (1994) *Nature (London)* 372, 44–45.
18. Bevan, M. J. (1977) *Nature (London)* 269, 417–418.
19. von Boehmer, H. (1990) *Annu. Rev. Immunol.* 8, 531–556.

20. Sykulev, Y., Cohen, R. J. & Eisen, H. N. (1995) *Proc. Natl. Acad. Sci. USA* 92, 11990–11992.
21. Schodin, B. A., Tsomides, T. J. & Kranz, D. M. (1996) *Immunity* 5, 137–146.
22. Valitutti, S., Müller, S., Cella, M., Padovan, E. & Lanzavecchia, A. (1995) *Nature (London)* 375, 148–151.
23. McKeithan, T. W. (1995) *Proc. Natl. Acad. Sci. USA* 92, 5042–5046.
24. Rabinowitz, J. D., Beeson, C., Lyons, D. S., Davis, M. M. & McConnell, H. M. (1996) *Proc. Natl. Acad. Sci. USA* 93, 1401–1405.
25. Hopfield, J. J. (1974) *Proc. Natl. Acad. Sci. USA* 71, 4135–4139.
26. Fersht, A. (1977) *Enzyme Structure and Mechanism* (Freeman, San Francisco), pp. 285–286.
27. Sykulev, Y., Brunmark, A., Jackson, M., Cohen, R. J., Peterson, P. A. & Eisen, H. N. (1994) *Immunity* 1, 15–22.
28. Yelton, D. E., Rosok, M. J., Cruz, G., Cosand, W. L., Bajorath, J., Hellström, I., Hellström, K. E., Huse, W. D. & Glaser, S. M. (1995) *J. Immunol.* 155, 1994–2004.

# The specificity of TCR/pMHC interaction

Markus G Rudolph and Ian A Wilson

Crystal structures of 11 complexes of TCRs with peptide/MHC (pMHC), that represent 6 independent TCRs, constitute the current structural database for deriving general insights into how  $\alpha\beta$  TCRs recognise peptide-bound MHC class I or class II. The TCRs adopt a roughly diagonal orientation on top of the pMHCs, but the identification of a set of conserved interactions that dictate this orientation is not apparent. Furthermore, the specific interaction of each TCR with its cognate pMHC partner is quite variable and also involves bound water molecules at the TCR/pMHC interface. In two of the systems, the structural basis for binding of altered peptide ligands has illustrated that the only significant conformational changes occur in the TCR/pMHC interface, but their small magnitude is inconsistent with the enormous variation in signalling outcomes. The TCRs adjust to different agonist, partial agonist and antagonist peptides by subtle conformational changes in their complementarity-determining regions, as previously observed in induced-fit mechanisms of antibody/antigen recognition. Allereactive-complex structures determined or modelled so far indicate increased interactions of the TCR  $\beta$ -chain with the pMHC compared with their syngeneic counterparts.

## Addresses

The Scripps Research Institute, Department of Molecular Biology, and The Skaggs Institute for Chemical Biology, 10550 North Torrey Pines Road, La Jolla, CA 92037, USA

Correspondence: Ian A Wilson; e-mail: wilson@scripps.edu

Current Opinion in Immunology 2002, 14:52–65

0952-7915/02/\$ – see front matter

© 2002 Elsevier Science Ltd. All rights reserved.

## Abbreviations

<b>APL</b>	altered peptide ligand
<b>BSA</b>	buried surface area
<b>CDR</b>	complementarity-determining region
<b>HV4</b>	hypervariable region 4
<b>pMHC</b>	peptide/MHC
<b>sc</b>	single-chain

## Introduction

Since determination of the first mouse and human TCR and TCR/pMHC (peptide/MHC) structures [1–3,4\*\*] in 1996 and soon afterwards, the expected flurry of new TCR structures and TCR/pMHC complexes has not materialised (Figure 1). Indeed, just four new independent TCR/pMHC complexes, two with MHC class I [5,6\*\*] and two with MHC class II [7,8\*\*], have been published in the past three years (Table 1). This situation attests to the continued difficulty in producing sufficient quantities of TCRs, either intact or as single-chain (sc) TCR Fv-like fragments, for crystallographic studies. In contrast, the number of MHC class I and class II crystal structures has been increasing dramatically (Figure 1), similar to the explosion in antibody structure determinations that began around 1989–1990. Although we have been able to derive

an enormous amount of information already from these six independent TCR/pMHC complexes, history tells us, when considering the antibody/antigen field [9], that not all key structural principles of TCR/pMHC recognition will be gleaned from these first few structures. Nevertheless, given the fact that  $\alpha\beta$  TCRs are restricted to MHC or MHC-like antigens, this situation may be mitigated compared with the almost infinite diversity that must be accounted for in antibody/antigen recognition.

In the past two years, the most significant advances in our understanding of TCR/pMHC interactions have come from the determination of three new TCR/pMHC complexes [6\*\*,7,8\*\*] that now include an MHC class I allogeneic complex and the first complexes with mouse and human MHC class II. In addition, several other complexes have been published with altered peptide ligands (APLs), which include strong agonists, weak agonists and antagonists for two systems — the human A6/HLA-A2 [10] and the mouse 2C/H-2K<sup>b</sup> [4\*\*]. Two allogeneic TCR/pMHC complexes [6\*\*,11\*] have illustrated that the general structural features seen in syngeneic complexes apply, although some surprises have come from one of these structures [6\*\*]. Finally, this past year produced the first structure of a  $\gamma\delta$  TCR [12\*\*] that now completes our structural view of primary antigen-recognition receptors — the antibody, the  $\alpha\beta$  TCR and the  $\gamma\delta$  TCR (Figure 2). These new crystal structures from 1999–2001 and the insights they brought are the focus of this review (Table 1). Other notable previous reviews on this subject include [13–20].

## Production of TCR/pMHC complexes

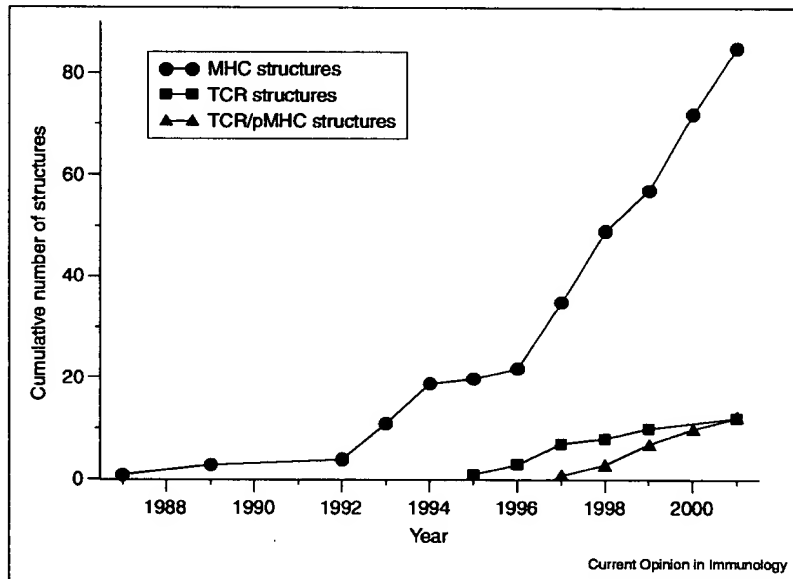
No general method has yet emerged for rapid production of sufficient quantities of soluble TCRs for crystallographic studies. In a previous review [13], we outlined some of the expression systems that were used to produce TCR protein for structural studies. Here, we will only briefly highlight novel features that facilitated production of TCR/pMHC crystals.

Most of the MHC molecules have been produced in *Escherichia coli* and refolded from inclusion bodies, except for murine H-2K<sup>b</sup> and HLA-DR1, which have also been produced in *Drosophila melanogaster* cells (Table 1). For MHC class II, the peptide is normally covalently attached through a linker to the amino terminus of the  $\beta$ -chain, in an innovative approach pioneered by Kappler and Marrack (see [21]). In another extraordinarily inventive approach, the peptide was covalently connected not to the MHC, but to the amino terminus of the  $\beta$ -chain of the TCR [8\*\*]. This construct was critical in obtaining stable complexes of human TCR HA1.7 with HLA-DR1 and HLA-DR4 that permitted their crystallisation [8\*\*,11\*]. This type of



**Figure 1**

Cumulative number of MHC, TCR and TCR/pMHC-complex crystal structures. The number of structures is plotted as a function of their deposition year in the Protein Data Bank (PDB) [72]. The plot does not contain structures that were superseded by re-determination at higher resolution. In order to avoid redundancy, the TCR and MHC structures in TCR/pMHC complexes are not included in the individual numbers. However, MHC and TCR complexes with other molecules, such as superantigens or antibodies, are included. For the TCRs, all fragments and constructs (such as single chains) that were determined by either X-ray diffraction or NMR spectroscopy are included. The first MHC crystal structure was determined in 1987 [36] and, after an approximately 5-year lag, the number of MHC structures increased dramatically, with as many as 15 structures added to the PDB in 2000. Compared with that, the number of new TCR and TCR/pMHC structures is lagging behind considerably.



stabilisation of complexes by reducing the (unfavourable) change in entropy during complex formation through covalent connection of binding partners has been successfully used previously, such as in scFvs [22], scTCRs [6\*,7] and the CD3 $\epsilon$  dimer [23\*].

These methods clearly have proven useful as a valuable general strategy to obtain homogenous samples for crystallisation. For the TCRs, intact extracellular domains have been produced both in *E. coli* and *D. melanogaster*, whereas scTCRs have been produced in both *E. coli* and myeloma cells. All of the relevant details on these expression constructs can be found in the primary references cited in Table 1.

### The $\gamma\delta$ TCR structure

Antibody structures were first determined in 1971 (see [24–26]), but it took another 25 years to visualise the intact  $\alpha\beta$  TCR structure [1,2]. Five years later (2001), we finally were presented with our first glimpse of a  $\gamma\delta$  TCR [12\*\*] to complement the V $\delta$  chain structure determined in 1998 [27]. This  $\gamma\delta$  TCR structure confirmed the view that these three sets of key antigen-recognition receptors have similar overall anatomies (Figure 2). The  $\gamma\delta$  TCR has often been called 'antibody-like', as compared with the  $\alpha\beta$  TCR, because of its ability to recognise intact proteins ([28]; reviewed in [29]) and in the correspondence of the lengths of their central complementarity-determining region (CDR)3 loops with antibodies rather than with  $\alpha\beta$  TCRs ([30]; reviewed in [31]). The study also described the putative binding site for phospho-antigens, for example pyrophosphates that are derived from mycobacteria [32,33].

### TCR/pMHC orientation

The six independent TCR/pMHC complexes (Table 1) show some fluctuation in the orientation that the TCR adopts on top of the pMHC (Figure 3a–c). This orientation was originally described as diagonal [1,2], but has recently been described for a class II TCR/pMHC complex as orthogonal [7]. However, it appears that the TCR orientation or twist on MHC class I and class II deviates about a relatively restricted mean that is currently spread by about 35° (Figure 3a), but that is still consistent with a generally diagonal orientation and footprint on the pMHC (Figures 3a and 4). However, as noted previously [5,34], the TCR deviates not only in its twist, but also in its roll (range 19°) and tilt (range 30°), which can be represented by the angle of inclination of the pseudo twofold axis between the V $\alpha$  and V $\beta$  domains relative to the MHC  $\beta$ -sheet floor (Figures 3b,c). In addition, the TCRs can differ in their  $\alpha\beta$  chain pairings, such that the pseudo V $\alpha$ /V $\beta$  twofold angle, which currently varies from 166° to 180°, can also contribute to the variation in TCR orientation on the pMHC.

In earlier structures, a relatively constant interaction of V $\alpha$  with the amino-terminal half of the peptide-binding groove was noted, as compared with the much more variable V $\beta$  interaction with the carboxy-terminal half (reviewed in [13]). This generalisation is still borne out in the recently described complexes, except for the allogeneic scBM3.3/H-2K<sup>b</sup>/pBM1 complex, where almost no direct contacts are observed between the V $\alpha$  chain and the pMHC (Figures 3c and 4). In the scBM3.3 structure, V $\alpha$  hovers just above the surface, creating a voluminous cavity that is occupied by ~30 water molecules [6\*\*]. Otherwise, considerably more variation occurs in V $\beta$  interactions with



Table 1

## Overview of TCR/pMHC complex structures 1996–2001.

Complex (TCR/MHC/peptide)	PDB ID	Peptide activity	Constructs and expression systems	References
<b>Class I</b>				
2C/H-2K <sup>b</sup> /dEV8	2ckb	Weak agonist	<i>D. melanogaster</i> , acidic/basic leucine zipper for specific TCR chain-pairing	[1,3]
2C/H-2K <sup>b</sup> /SIYR	1g6r	Superagonist*		[4**]
2C/H-2K <sup>b</sup> m3/dEV8	1jtr	Weak agonist		(a)
scBM3.3/H-2K <sup>b</sup> /pBM1	1fo0	Agonist	Myeloma cells for TCR, <i>E. coli</i> for MHC (refolded from inclusion bodies)	[6**]
B7/HLA-A2/Tax	1bd2	Strong agonist*	<i>E. coli</i> , refolded from inclusion bodies	[5]
A6/HLA-A2/Tax	1ao7	Strong agonist*	<i>E. coli</i> , refolded from inclusion bodies	[2]
A6/HLA-A2/TaxP6A	1qm	Weak antagonist		[10]
A6/HLA-A2/TaxV7R	1qse	Weak agonist		[10]
A6/HLA-A2/TaxY8A	1qsf	Weak antagonist		[10]
<b>Class II</b>				
scD10/I-A <sup>k</sup> /CA	1d9k	Agonist	<i>E. coli</i> for TCR, refolded from inclusion bodies; CHO cells for MHC. Peptide covalently connected to the MHC	[7]
HA1.7/HLA-DR1/HA	1fyt	Agonist	<i>E. coli</i> for TCR, refolded from inclusion bodies; <i>D. melanogaster</i> for MHC. Peptide covalently connected to the TCR	[8**]
HA1.7/HLA-DR4/HA	1j8h	Agonist		[11*]

\*The designation 'superagonist' or 'strong agonist' is equivalent in these instances. (a) JG Luz, M Huang, KC Garcia, MG Rudolph, L Teyton, IA Wilson, unpublished data. PDB ID, PDB identification number. sc, single-chain Fv fragment of the TCR. Only structures from 2000 onwards are annotated.

pMHC, as illustrated by the clustering of the tips of CDR1 $\alpha$  and CDR2 $\alpha$  loops, compared with the diversity in positioning of the equivalent CDR $\beta$  loops in different complexes (Figures 3a and 5).

### Analysis of the TCR/pMHC interactions

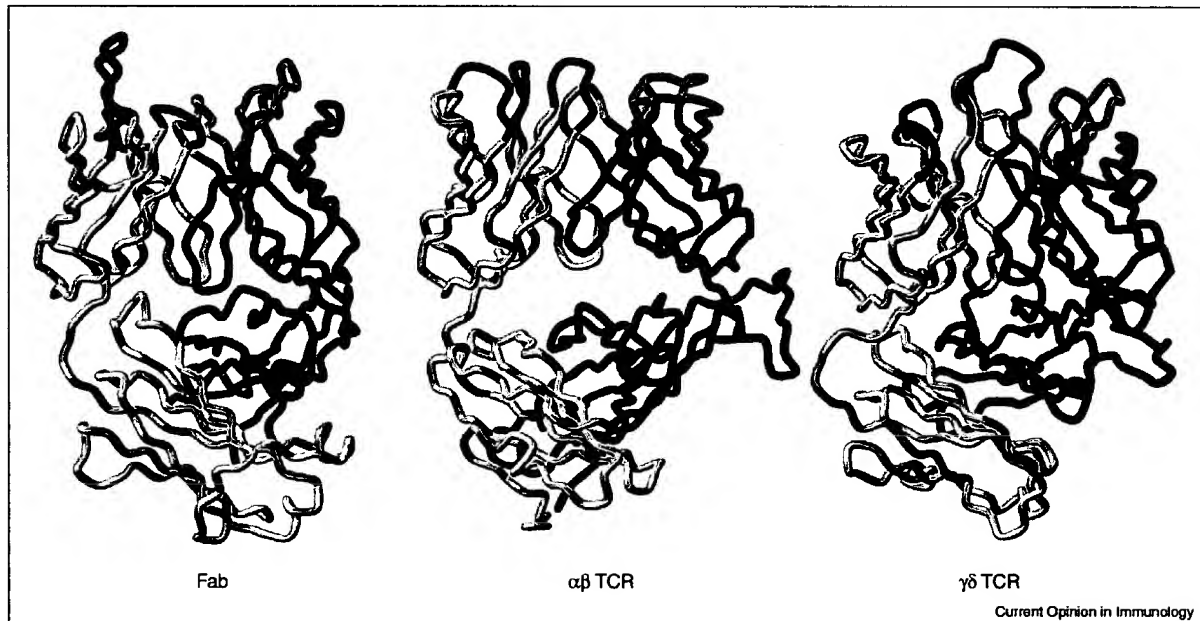
Eleven TCR/pMHC complex structures have been published (or the results are 'in press') during the past five years (Table 1). A detailed analysis of these complexes, that includes comparison of buried surface area (BSA) at the TCR/pMHC interface, and the contributions to the interface of peptide versus MHC, of V $\alpha$  versus V $\beta$  and of the individual CDR loops, is given in Table 2. The BSA for the TCR/pMHC complex varies extensively — between 1239 Å<sup>2</sup> and 1931 Å<sup>2</sup>. The percentage contribution of the peptide to the pMHC side of that interface is more narrowly confined to a range of 21%–34%, whereas V $\alpha$  has contributed from 37%–74% (average 57%) and, conversely, V $\beta$  from 26%–63% (average 43%) of the TCR buried surface. A similar bias in chain usage has been noted for antibodies, where V<sub>H</sub> usually provides a larger contribution to the antibody/antigen interface [9].

An extraordinary amount of variation also occurs in the contribution of individual CDR loops to their respective

TCR/pMHC interfaces. For V $\alpha$ , the percentage contribution of its CDRs 1–3 to the buried surface varies from an average of 21% for CDR1 $\alpha$  (range 14%–29%), to 12% for CDR2 $\alpha$  (8%–17%), and to 21% for CDR3 $\alpha$  (6%–27%). Hypervariable region 4 (HV4) makes relatively little percentage contribution to either the  $\alpha$  chain (0–11%) or the  $\beta$  chain (0–2%) interface, but could still contribute key orienting contacts or electrostatic interactions (see below). For V $\beta$ , the equivalent values are more extreme, with average contributions for CDR1 $\beta$  being 6% (0–16%), 11% for CDR2 $\beta$  (0–23%) and 24% for CDR3 $\beta$  (10%–39%). In some instances, CDRs 1 $\beta$  and 2 $\beta$  actually contribute little (or nothing) to the TCR/pMHC buried surface, as for complexes of TCRs A6 and B7 with HLA-A2.

In fact, when one analyses the actual number of contacts rather than the buried surface (Table 2, bottom), CDR1 $\beta$  and CDR2 $\beta$  often make minimal contact with the pMHC compared with CDR3 $\beta$ . For V $\alpha$ , this trend mainly applies to CDR2 $\alpha$ , although it is much less pronounced, except for the allogeneic scBM3.3 complex where CDR3 $\alpha$  has almost no contacts. Thus, in most cases, the centrally located CDR3 loops dominate the interactions with pMHC.

Figure 2



Overall comparison of the anatomy of antibody Fab,  $\alpha\beta$  TCR and  $\gamma\delta$  TCR structures. Light-grey shading is used for the antibody light (L) chain and TCR  $\alpha$  or  $\delta$  chains; dark-grey shading is used for the antibody heavy (H) chain and TCR  $\beta$  or  $\gamma$  chains. The CDR loops are

colour-coded as follows: for the L,  $\alpha$  and  $\delta$  chains, CDR1 is dark blue, CDR2 is magenta and CDR3 is green; for the H,  $\beta$  and  $\gamma$  chains, CDR1 is cyan, CDR2 is pink, CDR3 is yellow and HV4 is orange (TCRs only).

### The contribution of the bound peptide to TCR interactions

How much does the peptide itself contribute to the pMHC interface? How can the TCR distinguish one peptide from another, when presented by the same MHC molecule? Many immunological studies (e.g. [35]) prior to the determination of a TCR/pMHC structure — combined with the plethora of pMHC structures that first originated from the HLA-A2 structure in 1987 [36] and subsequent single-peptide/pMHC complexes in 1992 [37–39] — suggested that a few up-pointing side-chains of the peptide would be the major determinants that contribute to the specificity of the TCR/pMHC interaction.

#### Physiological ligands

The TCR/pMHC crystal structures have graphically cemented that view, where usually only 2–5 peptide side-chains are involved in direct TCR contact (Table 3). In MHC class I, these interactions are dominated by the peptide residues that bulge most out of the groove and, hence, represent functional hotspots [4\*\*] in the TCR/pMHC interface. For nonamer and octamer peptides, these represent predominantly residues P5, P7 and P8, and P4, P6 and P7, respectively. For MHC class II peptides, the key side-chain contributions are more uniformly dispersed (predominantly P-1, P2, P3, P5 and P8) due to the extensive backbone interactions in the class-II

binding groove that confine their structures to repeating polypyrrolone type-II helix-like conformations [40]. In class II, the peptides also lie slightly deeper in the MHC binding groove (Figure 3d).

Clearly, the peptide is able to dominate the TCR/pMHC interface more in MHC class I due to the differential ability to bulge out of the groove depending on the length of the peptide and the polymorphic residues that line the MHC peptide-binding groove [41\*\*]. Extensive ridges in some MHCs force the peptide to bulge even higher out of the groove and provide more intimate contact with the TCR [42,43]. On the other hand, the contribution of the peptide backbone to TCR interaction is very modest for both MHC class I and class II, where none, or only a handful of, contacts are made (Table 3, bottom). The only exception so far is for the HLA-A2/Tax complex, where the large P4–P5 bulge includes a glycine at P4 that enables the TCR to more easily access the peptide backbone (Figure 3d).

#### Altered peptide ligands

So far, no dramatic structural changes that could account for the magnitude of the different signalling outcomes of various APLs have been noted in the TCR/pMHC structures, when strong agonist, weak agonist and antagonist peptides are presented by the same MHC to the same TCR [4\*\*,10]. Only slight readjustments occur in the TCR/pMHC interface to

Table 2

## Crystal structures and analysis of TCR/pMHC-class-I complexes.

TCR	2C	2C	scBM3.3	B7	A6	A6	A6	A6	scD10	HA1.7	HA1.7	Average
MHC	H-2K <sup>b</sup>	H-2K <sup>b</sup>	H-2K <sup>b</sup>	HLA-A2	HLA-A2	HLA-A2	HLA-A2	HLA-A2	I-A <sup>k</sup>	HLA-DR1	HLA-DR4	values
Peptide	dEV8	SIYR	pBM1	Tax	Tax	TaxP6A	TaxV7R	TaxY8A	CA	HA	HA	
Resolution (Å)	3.0	2.8	2.5	2.5	2.6	2.8	2.8	2.8	3.2	2.6	2.4	–
BSA (Å <sup>2</sup> )	1891	1795	1239	1651	1801	1767	1753	1666	1733	1931	1915	1740
<b>% Contribution to buried surface</b>												
Peptide	24	24	21	32	34	33	34	27	23	33	32	29
V <sub>α</sub>	54	52	37	67	64	66	64	74	61	46	47	57
CDR1	23	18	14	28	25	23	23	29	22	15	15	21
CDR2	13	16	17	13	10	13	10	12	15	8	9	12
CDR3	16	16	6	23	25	25	26	27	22	22	23	21
HV4	2	0	0	0	4	11	6	7	1	0	0	3
V <sub>β</sub>	46	48	63	33	36	34	36	26	39	54	53	43
CDR1	16	15	10	0	2	2	2	0	3	8	8	6
CDR2	17	21	14	11	0	1	0	0	13	23	16	11
CDR3	10	11	39	22	33	31	34	26	16	22	23	24
HV4	1	2	1	0	0	0	0	0	0	1	1	1
<b># Contacts</b>												
MHC	63	39	60	46	76	76	90	82	98	84	82	72
Peptide	23	35	34	60	47	60	58	30	34	37	34	41
Total	86	74	94	106	123	136	148	112	132	121	116	113
V <sub>α</sub>	69	40	29	72	74	98	96	88	70	46	51	67
CDR1	23	19	11	25	24	23	21	23	28	13	16	21
CDR2	17	1	16	17	3	4	8	9	16	2	5	9
CDR3	26	20	2	30	41	60	56	49	23	30	29	33
HV4	3	0	0	0	6	9	5	7	2	0	0	3
V <sub>β</sub>	17	34	65	34	49	38	57	24	62	75	66	47
CDR1	7	16	1	0	3	4	4	0	0	15	13	6
CDR2	6	2	9	3	0	0	0	0	31	28	17	9
CDR3	4	15	55	31	46	34	53	24	24	22	25	30
HV4	0	0	0	0	0	0	0	0	0	0	0	0

BSA was calculated with MS [73] using a 1.7 Å probe radius. Contacts were calculated with HBPLUS [74] and CONTACSYM [75].

accommodate different up-pointing peptide side-chains. In the A6 system, the number of peptide/TCR contacts does not correlate with the degree of agonism and antagonism (Table 3), although there is a slight, but probably insignificant, increase in the overall BSA for the strong agonist, Tax (Table 2). Similarly, in the 2C system [4\*\*], the BSA does not change much, but the complementarity and the number of TCR/pMHC contacts increases despite the relatively minor substitution of an arginine (in the strong agonist, SIYR) for a lysine (in the weak agonist, dEV8) at P4 (Table 3). Again, no gross conformational changes in the TCR or pMHC are observed, but slight rearrangements in the CDR loops accommodate the different peptides (Figure 5b), as particularly exemplified by the conformational adjustments seen in the CDR3β loop in the A6 TCR on binding different pMHCs (Figure 5c).

The correlation between the half-life of a complex [44] and the degree of agonism or antagonism is also not clear-cut. In both

2C and A6, the strong agonists (SIYR and Tax) have a longer half-life (9.2 s and 7.5 s) than weak agonists (3.7 s for H-2K<sup>b</sup>/dEV8 and 1.5 s for HLA-A2/TaxV7R). However, by using surface plasmon resonance (SPR), agonists have been found in the A6 system that have shorter half-lives than antagonists [45\*]. In this study, an antagonist was converted to an agonist by stepwise filling of a cavity in the TCR/pMHC interface and the biological activity paralleled the TCR/pMHC affinity, not the half-life of the complex [45\*]. So questions arise as to whether these SPR measurements using soluble receptors really represent what is happening on the cell surface. Longer half-lives of TCR/pMHC complexes on the cell surface could lead to additional stabilisation by the co-receptors CD4 and CD8 [46]. Although solution studies yielded contradictory results for TCR/pMHC oligomerisation [47,48], lateral interactions among the TCR/pMHC signalling complexes or interactions with other co-stimulatory or inhibitory receptors, as in the immunological synapse, may only form above a certain threshold of TCR/pMHC-complex half-life [49].

### Positive selection and TCR bias

A question that we have been specifically asked to address with respect to the current set of TCR/pMHC crystal structures is how positive selection on self-pMHC molecules produces a repertoire highly biased to effective recognition of unknown foreign peptides bound to the same allelic form of an MHC molecule.

This question could be restated to ask how it is that positively selected T cells retain sensitivity to peptides they encounter in the periphery. Clearly, foreign peptides are not really any different from self-peptides and, indeed, some may be antagonists as well as agonists. Which ones are which depends on the complementarity of their interaction with the TCR in the context of the pMHC. The conserved docking mode of the TCR on the pMHC offers some explanation for how a collection of different peptides — the peptide repertoire — is recognized in the context of the same MHC. The same interactions that steer the TCR towards its generally diagonal orientation place the CDR1 and CDR2 loops over the long  $\alpha 1$  and  $\alpha 2$  ( $\beta 1$ ) helices of the MHC class I (II) molecule. Indeed, given the more conserved interactions for the V $\alpha$  CDR1 and CDR2 loops with pMHC that have been shown so far, the V $\alpha$  domain would appear to be more critical in determining the orientation and hence in setting up the readout of the peptide sequence. These relatively conserved germline CDR1 and CDR2 interactions [13] provide the basic affinity of the TCR for the generic MHC allele, where the CDR3 loops are positioned to primarily contact the peptide.

Various mutagenesis experiments have shown that no single contact or set of contacts dominates the TCR/pMHC interaction [50], contrary to what is often observed in antibody/antigen interactions, where somatic mutation can allow a small number of high-affinity interactions to dominate the energy landscape [51]. For TCRs, if the affinity (or half-life) of the complex in the thymus becomes too high (or long) due to excessive interactions with the peptide, negative selection will occur.

Thus, interaction of the CDR1 and CDR2 loops with the MHC-helices, or even the peptide backbone, is likely to be responsible for positive selection, whereas the CDR3 loops play a more important role in negative selection. The latter leads directly to priming of the TCRs for sensitivity against any peptide encountered in the periphery: CDR1 and CDR2 loops provide for basal affinity, and CDR3 loops for specificity. Again, lack of any somatic mutation in the TCRs that would drive high-affinity engagement allows the TCR to be relatively permissive for substitutions of peptide side-chains in the interface. Certain key positions in the peptide, usually those that protrude highest from the groove, provide the basis for discrimination of peptide and for altering the affinity or half-life of the TCR/pMHC interaction. As described for the 2C system [4\*\*], the central P4 and P6 up-pointing residues form a

functional 'hotspot' around which the TCR is highly sensitive to changes in the particular peptide residues.

Furthermore, in some linked examples of alloreactive complexes, substantial bulging of the peptide out of the groove may dominate the interaction so as to allow cross-reactivity with 'foreign' MHC that may even disrupt the standard V $\alpha$  interactions [6\*\*]. In normal situations, the generally diagonal orientation places the CDR3 loops in the center of the groove where, for class I peptides, substantial bulging of the peptide backbone or protrusion of the central peptide side-chains can arise. The curvature of two interacting globular surfaces of the TCR and pMHC leads to greater distances between the peptide at the amino terminus, and to some extent at the carboxyl terminus, than in the middle, again explaining the sensitivity of the central CDR3 loops to reading-out the central peptide sequence. For class II peptides, the central P1–P9 residues are of more constant depth and do not rise towards the TCR except at their ends.

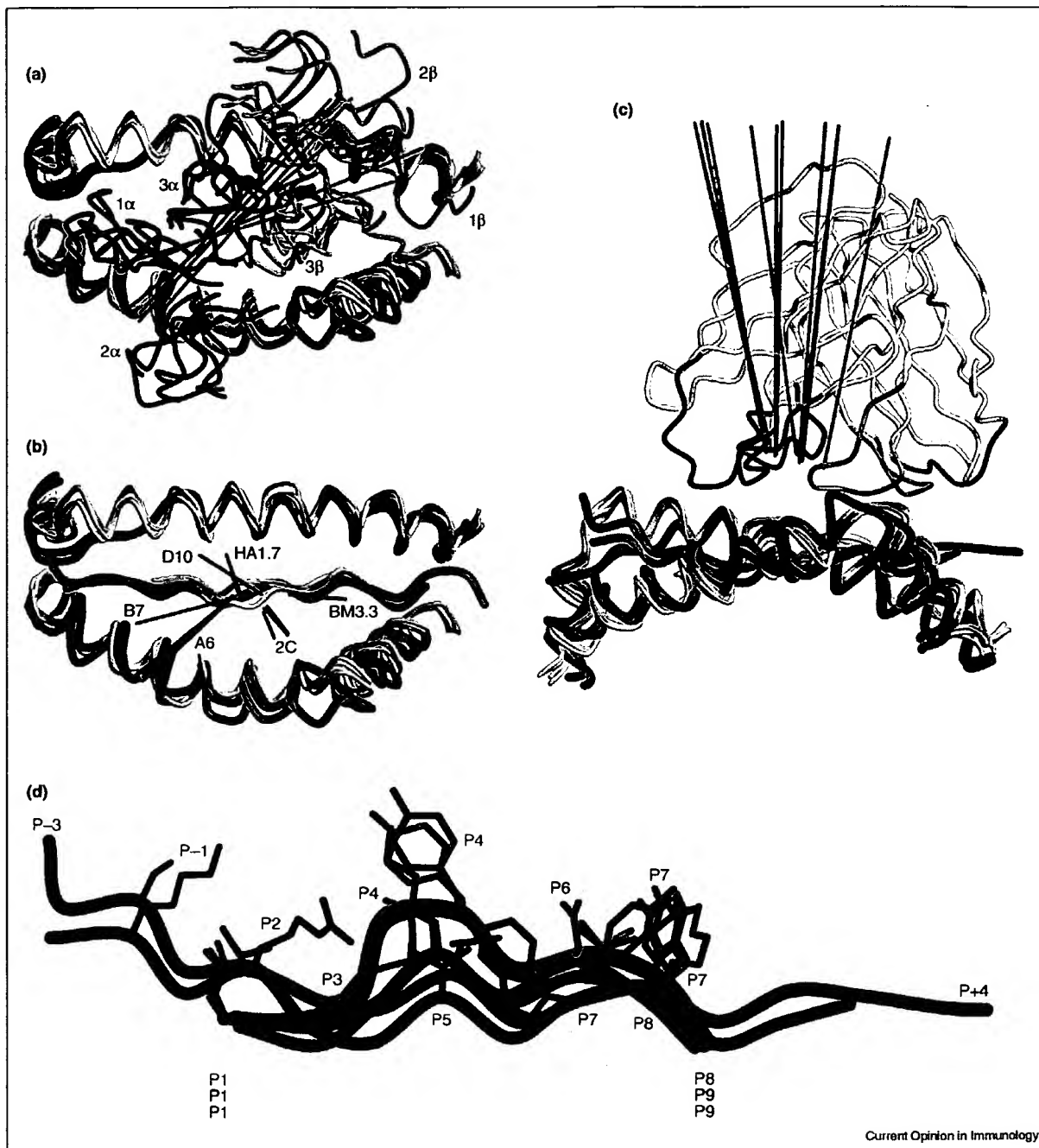
Such effects are tabulated in Table 3 where, for class I, the main peptide contribution to TCR recognition are at P5, P7 and P8 for nonamers, and P4, P6 and P7 for octamers. For class II, the corresponding residues are P5 and P8, but P2 also becomes a player, because its backbone interaction with the class II MHC raises the amino end of the class II peptide out of the groove in relation to the more deeply embedded amino end of the class I peptides. The greater conservation of the TCR  $\alpha$  chain interaction and location in the syngenic complexes determined so far suggests that the  $\alpha$  chain may play a more important role in setting up the initial pMHC interaction, whereas the  $\beta$  chain then is able to adapt to fit whatever is encountered in the form of peptide at the carboxy-terminal half of the groove.

### Alloreactivity

Alloreactivity may occur in response to the polymorphic variation in the MHC or in selection of a different peptide repertoire as a result of these 'mutated' residues in the MHC. So far, three complexes have been used to address this issue ([6\*\*,11\*]; JG Luz, M Huang, KC Garcia, MG Rudolph, L Teyton, IA Wilson, unpublished data).

The complex of the scBM3.3 TCR with the allogeneic MHC H-2K<sup>b</sup> is perhaps the most structurally distinct so far, but the corresponding syngenic complex is currently not known. The scBM3.3 TCR tilts substantially towards the  $\beta$ -chain side (Figures 3c and 4), with the  $\alpha$ -chain making few direct contacts with the MHC (Table 2). In fact, the long central CDR3 $\alpha$  is flared back such that it makes no contacts with the peptide and only two with the MHC (Table 2). The majority of the interactions are with the  $\beta$ -chain, consistent with that proposed for the interaction of H-2L<sup>d</sup> with TCR 2C, where an extreme bulge in the carboxy-terminal half of the peptide is likely to increase its interaction with the TCR  $\beta$ -chain [43]. Two recent structural studies ([11\*]; JG Luz, M Huang, KC Garcia,

Figure 3



Current Opinion in Immunology

MG Rudolph, L Teyton, IA Wilson, unpublished data) confirm that subtle changes in allogeneic MHCs may alter the peptide conformation and location such that the same peptide is presented differently to the TCR. Thus, these structural studies conclude that TCR interaction with the bound peptide strongly affects the alloresponse.

#### TCR conformational variation and changes

Sufficient numbers of TCR structures are now available to assess the extent of conformational variation that arises in their antigen-combining sites (Figure 5a). As expected, the four TCR outer CDRs 1 and 2 adopt canonical conformations [52\*], as first described for antibodies [53,54]. A small



**Figure 3 legend**

Relative orientation of the TCR on top of the MHC and comparison of peptide conformations in TCR/pMHC (class I versus class II) complexes. The MHC helices are shown as light and dark grey tubes for class I and class II, respectively. The CDR loops are coloured as in Figure 2. Lines and axes are coloured blue for class II TCRs and orange and red for human and mouse class I TCRs, respectively. (a) Variation in the diagonal (twist) orientation of the six independent TCR/pMHC complexes. The projection of a linear least-squares fit through the centres of gravity of the CDR loops is shown for the six different TCRs. (b,c) Variation in the tilt and roll of TCR/pMHC complexes. The pseudo two-fold axes (colour code as above) that relate the  $V\alpha$  and  $V\beta$  domains of the TCRs to each other are shown for twelve TCR/pMHC structures of six different TCR molecules (scD10, HA1.7, B7, A6, 2C and

scBM3.3). This gives a good estimate of the inclination (roll, tilt) of the TCR on top of the MHC, which is a function of the TCR, not the pMHC ligand. One extreme case is the allogeneic scBM3.3 TCR, which is shown as a transparent  $C\alpha$  trace in the side view of (c). (d) The  $C\alpha$  traces of the bound peptides (removed from their respective MHCs) are drawn as tubes with the TCR-contacting side-chains (see Table 3) as stick representations. Only a representative peptide for each of the six independent TCR/pMHC complexes is shown (Table 1). Class-I-bound peptides from mouse and human are coloured red and green, respectively. Peptides from class II complexes are coloured blue. The peptides are oriented with their TCR-contacting residues pointing upward. The  $\beta$ -sheet floors of the peptide-binding sites of the MHC molecules were superimposed to align the peptides.

number of discrete canonical conformations may be able to describe most of the known sequences of the  $\alpha 1,2$  and  $\beta 1,2$  loops. At present, 3–4 canonical structures have been

defined for each of these loops [52]. What makes the TCR different from antibodies is the enormous variation seen in both of the central CDR3s (Figure 5a). In antibodies,

**Table 3****Interactions of the peptide component of the pMHC with the TCR.**

TCR/MHC/peptide	#Peptide residues	Peptide residue (P) and # contacts per residue												Total # contacts
<b>Peptide side-chain contacts with TCR</b>														
<b>Human class I</b>														
A6/HLA-A2/Tax	9			P1	P2	P3	P4	P5	P6	P7	P8	P9		
A6/HLA-A2/TaxP6A	9			1	–	–	–	15	1	5	11	–		33
A6/HLA-A2/TaxV7R	9			–	–	–	–	27	–	5	12	–		44
A6/HLA-A2/TaxY8A	9			1	–	–	–	19	–	11	14	–		45
B7/HLA-A2/Tax	9			4	–	–	–	15	–	1	–	–		20
	9			4	–	–	–	29	–	4	10	–		47
<b>Mouse class I</b>														
scBM3.3/H-2K <sup>b</sup> /pBM1	8			P1	P2	P3		P4		P5	P6	P7	P8	
2C/H-2K <sup>b</sup> /dEV8	8			–	–	–		1		–	20	8	–	29
2C/H-2K <sup>b</sup> /SIYR	8			–	–	–		18		–	3	2	–	23
	8			–	–	–		14		–	21	–	–	35
<b>Human/mouse class II</b>														
		P–2	P–1	P1	P2	P3	P4	P5	P6	P7	P8	P9	P+1	
scD10/I-A <sup>k</sup> /CA	16	–	1	–	11	–	–	8	–	4	7	–	–	31
HA1.7/HLA-DR1/HA	13	–	6	–	2	4	1	6	–	–	8	–	–	27
HA1.7/HLA-DR4/HA	13	–	4	–	4	5	–	3	–	–	8	–	–	24
<b>Peptide main-chain contacts with TCR</b>														
<b>Human class I</b>														
A6/HLA-A2/Tax	9			P1	P2	P3	P4	P5	P6	P7	P8	P9		
A6/HLA-A2/TaxP6A	9			–	1	–	10	–	1	1	1	–		14
A6/HLA-A2/TaxV7R	9			–	1	–	11	–	2	1	1	–		16
A6/HLA-A2/TaxY8A	9			–	1	–	10	1	–	–	1	–		13
B7/HLA-A2/Tax	9			–	1	–	9	–	–	–	–	–		10
	9			–	–	–	5	–	1	4	3	–		13
<b>Mouse class I</b>														
scBM3.3/H-2K <sup>b</sup> /pBM1	8			P1	P2	P3		P4		P5	P6	P7	P8	
2C/H-2K <sup>b</sup> /dEV8	8			–	–	–		–		–	2	3	–	5
2C/H-2K <sup>b</sup> /SIYR	8			–	–	–		–		–	–	–	–	–
<b>Human/mouse class II</b>														
		P–2	P–1	P1	P2	P3	P4	P5	P6	P7	P8	P9	P+1	
scD10/I-A <sup>k</sup> /CA	16	–	–	–	–	–	–	–	1	1	1	–	–	3
HA1.7/HLA-DR1/HA	13	–	–	–	–	–	–	1	2	1	3	–	–	7
HA1.7/HLA-DR4/HA	13	–	–	–	–	–	–	–	1	2	4	–	–	7

There are no TCR contacts with peptide residues P3 or P9 in any class I complex, whereas no TCR contacts are observed for peptide residues P1, P9 (P8 for octamers), or P+1 in any class II complex. All interactions were

calculated with HBPLUS [74] and CONTACTSYM [75] using standard van der Waals radii and a probe radius of 1.7 Å. The Tax peptide residue P4 is a glycine, which may explain its accessibility for main-chain contacts.

Figure 4

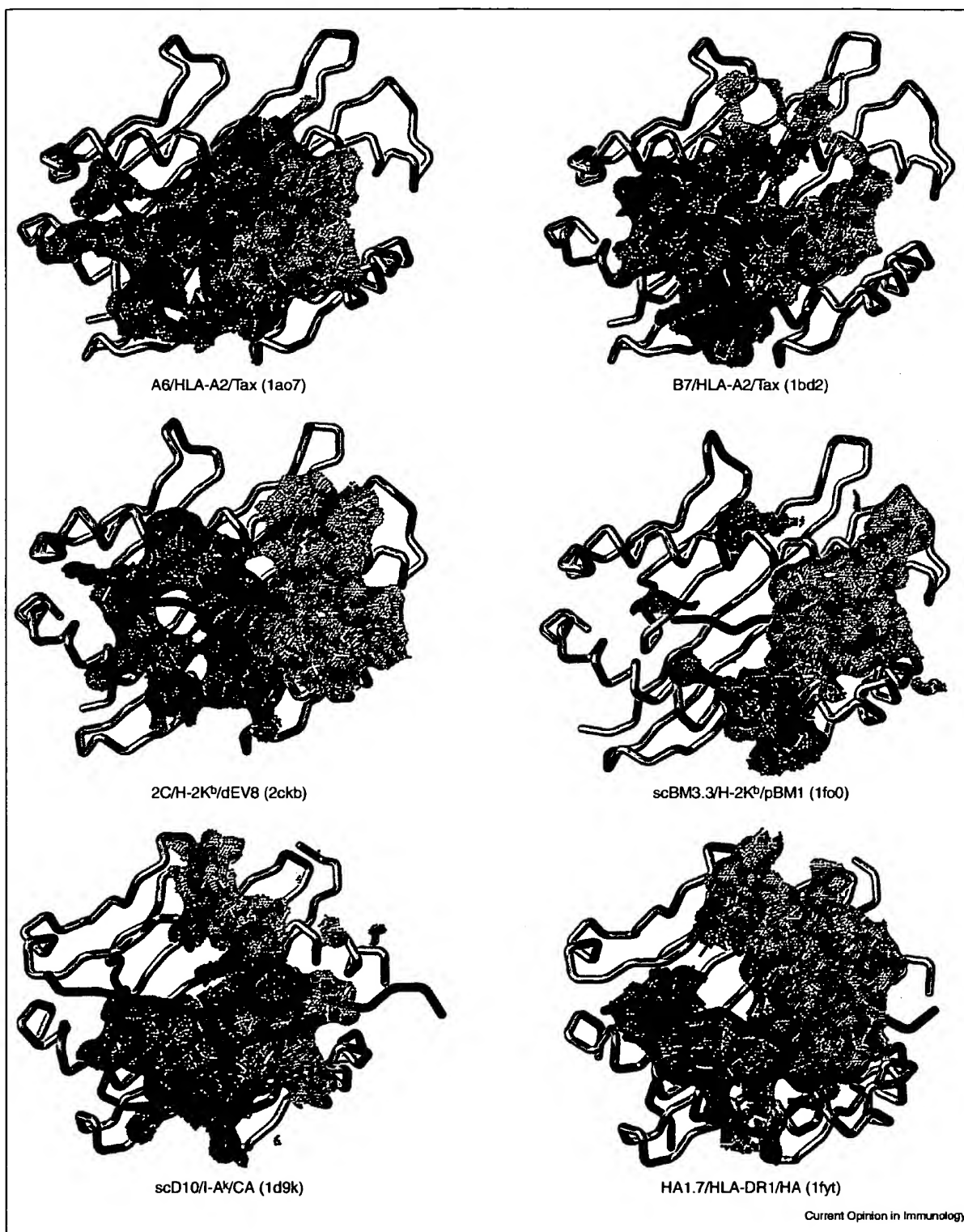


**Figure 4 legend**

Relative contributions of the TCR V $\alpha$  and V $\beta$  domains to the BSA of TCR/pMHC complexes. The view is from the TCR onto the peptide-binding site of the MHC. Peptide and MHC C $\alpha$  traces are shown as red and grey tubes, respectively. The surface buried by

the TCR V $\alpha$  (dark blue) and V $\beta$  (cyan) domains on the pMHC is represented as dots. Note the substantially reduced direct contacts of V $\alpha$  with the pMHC in the allogeneic scBM3.3/H-2K<sup>b</sup>/pBM1 complex.

CDR L3 adopts a well-defined set of canonical structures, but the equivalent CDR3 $\alpha$  loop is, in fact, the most variable in the current set of TCR structures. Thus, the prediction [55] that these central CDRs would be most variable and adapt to the pMHC primarily (but not exclusively [6\*\*]) through contact with the peptide has been borne out.

Induced fit has also been addressed for TCRs as it was for antibodies [9]. Only one published example of free and bound TCRs is available for the 2C TCR [1,3], where substantially different conformations are seen for CDR1 $\alpha$  and CDR3 $\alpha$ . What has yet to be resolved is whether any of the CDRs can change their canonical structures upon pMHC binding. In antibodies, these CDRs, including CDR L3, usually only go through segmental shifts in structure (~1 Å–3 Å) that change their location, but not their overall shape [9,54,56]. The prediction is that TCRs will also conform to that notion [52\*] and, in fact, the tip of the TCR 2C CDR1 $\alpha$  loop moves in a hinge motion by 17°, without changing its overall shape (Figure 5b). For the central CDRs, it is more likely that these loops will also rearrange on ligand binding, as seen especially for the CDR H3 loops of antibodies [9].

Two examples are available to assess the extent of conformational variation in the CDR loops in the presence of an APL. For TCR 2C, only small variations are seen in CDR3 $\beta$  (Figure 5b) but, for TCR A6, these conformational rearrangements are much larger (Figure 5c). Evidence for flexibility in the TCR has also been derived from kinetic and thermodynamic studies [57–59]. Whether these data support a model in which flexible CDRs stabilise or rearrange upon pMHC binding remains an unanswered question. What is certainly consistent so far in both the structural and kinetic/thermodynamic experiments is that conformational rearrangements of the CDRs can provide better complementarity of the TCR to both the MHC [3] and the peptide [4\*\*,10].

**The role of bound water**

Several TCR/pMHC complexes contain bound water molecules in their TCR/pMHC interfaces. The ability of water molecules to provide additional complementarity by the filling of cavities in the interface is well documented for antibodies [60]. The highest resolution TCR/pMHC complexes (2.4 Å–2.5 Å; Table 2) contain 17 (2C/H-2K<sup>b</sup>m3/dEV8 [JG Luz, M Huang, KC Garcia, MG Rudolph, L Teyton, IA Wilson, unpublished data]), 39 (scBM3.3/H-2K<sup>b</sup>/pBM1 [6\*\*]) and 15 (HA1.7/HLA-DR4/HA [11\*]) waters in their

interface with 6, 12 and 6, respectively, mediating contact between the TCR and pMHC. No specific waters are conserved among these structures, indicating that their presence is dependent on the individual sequences of both the TCR and pMHC. In the allogeneic scBM3.3 complex, ~30 interfacial waters are sequestered in a cavity between the V $\alpha$  and the pMHC, as a result of the TCR V $\alpha$  domain lifting up (Figure 4) from the pMHC surface [6\*\*].

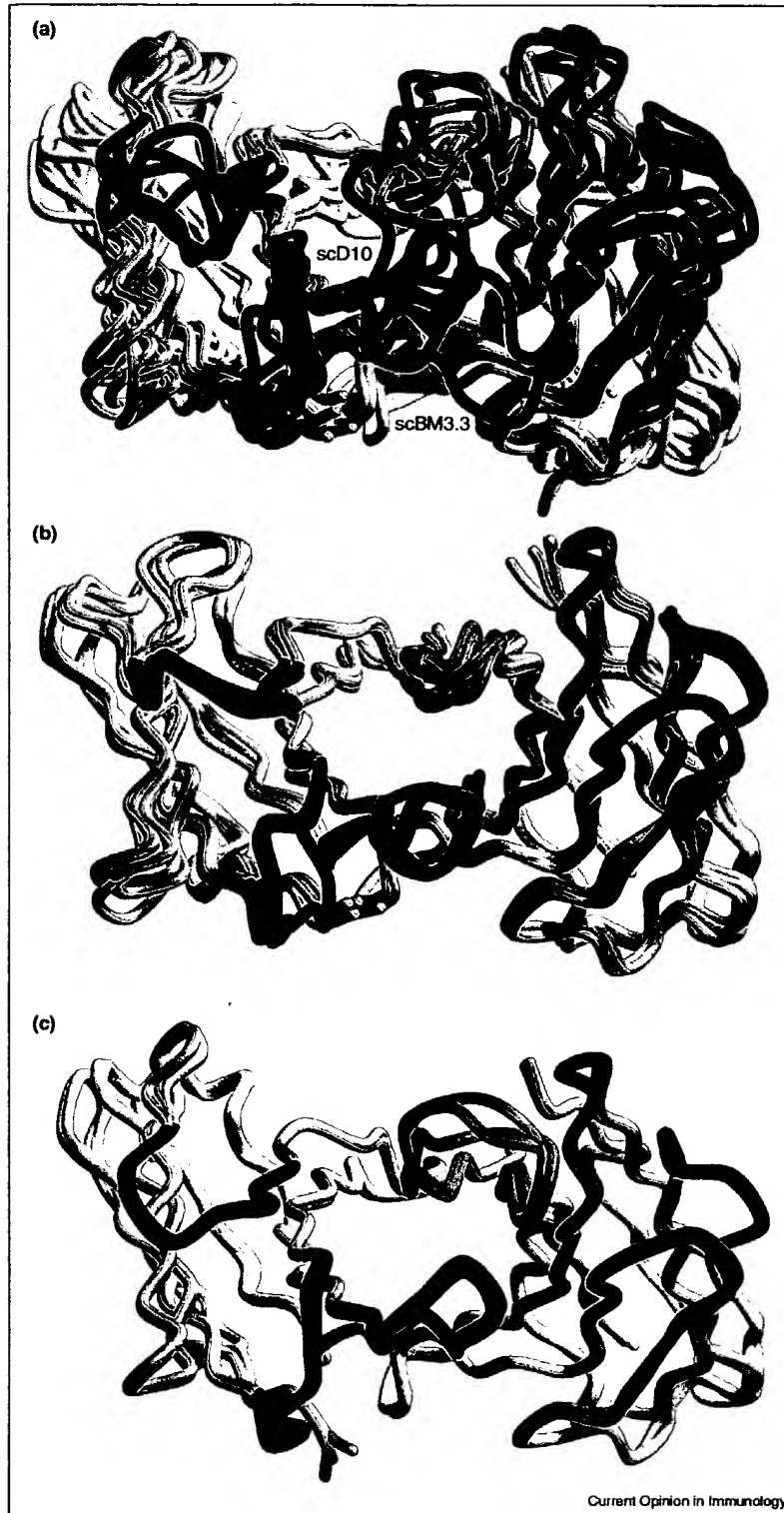
Thus, these recent, higher resolution TCR/pMHC structures indicate a strong involvement of bound water to provide complementarity and specificity to the recognition process. Indeed, small sequence and structure changes in either the peptide (APLs) or the MHC (as in alloreactive complexes) can be amplified on the pMHC surface by redistribution or acquisition of bound waters in the TCR/pMHC interface. A particularly good example of the role of waters in adding complementarity to pMHC interactions is found for the allogeneic H-2K<sup>b</sup>m8 complex, where water can partially substitute for loss in buried side-chain functional groups [61\*]. In addition, such buried MHC substitutions, which occur frequently in allogeneic MHC, can transmit their effects by altering the water structure and the electrostatic properties on the surface, even though their mutated residues are not directly 'seen' by the TCR ([11\*]; JG Luz, M Huang, KC Garcia, MG Rudolph, L Teyton, IA Wilson, unpublished data).

The release of bound waters upon TCR/pMHC complex formation increases the entropy and thus may also contribute favourably to the binding energy. In the 2C system, it is estimated that the TCR must displace at least 15 ordered water molecules from the pMHC, mainly by the outer CDR1 and 2 loops of both V $\alpha$  and V $\beta$  (JG Luz, M Huang, KC Garcia, MG Rudolph, L Teyton, IA Wilson, unpublished data) that primarily contact the MHC. However, due to the paucity of (high resolution) structural examples and the lack of biochemical data, it is difficult to assess the generality or extent of the contribution of water to the TCR/pMHC binding energetics.

**Conclusions and future perspectives**

The completion of a  $\gamma\delta$  TCR structure has finally enabled visualisation of the complete arsenal of primary antigen-recognition receptors. These receptors are remarkably similar in the overall structure of their antigen-binding domains (Figure 1) but, in the case of the  $\alpha\beta$  TCR, have become specialised to interact primarily with MHC or MHC-like molecules that can present peptides, lipids or glycolipid fragments [62] for immune surveillance.

Figure 5



Structural comparison of  $\alpha\beta$  TCRs. (a) Overlay of the V $\alpha$ /V $\beta$  domains of six different  $\alpha\beta$  TCRs from TCR/pMHC structures. The CDR and HV4 loops are coloured as in Figure 2. The central CDR3 loops are the most structurally diverse and recognise mainly the peptide whereas the CDR1 and CDR2 loops recognise the mostly conserved structural features on the MHC. The two most divergent CDR3 $\alpha$  loops are labelled and belong to MHC class I (scBM3.3)- and class II (scD10)-restricted TCRs. (b) Overlay of the unliganded 2C TCR with the three liganded structures. The unliganded 2C TCR structure shows significant conformational differences of both its CDR3 $\alpha$  loop (light green) and CDR1 $\alpha$  loop (furthest right of the dark blue loops). (c) Overlay of the four liganded A6 TCR structures. The A6 CDR3 $\beta$  loop (yellow) shows some conformational variability in response to the different Tax-peptide mutants in the HLA-A2 complexes.

What is most remarkable is the evolution of a common docking mode that enables the  $\alpha\beta$  TCR to survey the contents of the MHC binding-groove. It is not the common binding orientation that is in itself remarkable, but that the six independent complex-structures determined so far have not yet revealed the basis for this conserved orientation. No absolutely conserved pairs of interactions are apparent in these different TCR/pMHC-complex interfaces that would account for their relatively fixed docking orientations, especially when one considers the extreme variability in the V $\beta$  interactions with different pMHCs.

The variability in the tilt, twist and roll of the TCR indicates that individual solutions to the docking problem differ in the details in order to provide sufficient complementarity for binding (i.e. a  $K_d$  in the  $\mu$ M range) and, thus, for signalling. In most cases, the TCR V $\alpha$  interactions with the MHC seem to predominate and, hence, provide some basis for a conserved orientation. But the alloreactive scBM3.3 TCR is inconsistent with that generality, as most of its interactions with pMHC are due to the  $\beta$ -chain. However, some fortuitous interactions not present in the syngeneic complex may have altered the relative distribution of its interactions. Additionally, glycosylation may play a role in facilitating docking, as both the TCR and MHC are highly glycosylated which, hence, could sterically restrict the range of possible orientations [16,19].

Electrostatic interactions could also help pre-orient the TCR and pMHC. In TCRs, Lys68 in HV4 $\alpha$  is close to a negatively charged residue (Asp76 $\beta$  in MHC class II or Glu166 $\alpha$  in MHC class I) and may provide some orientation effects [63]. Although salt bridges and hydrogen bonds between these residues have not been conserved in all TCR/pMHC class I complexes (with variable distances of 2.9 Å–10 Å between the side-chain functional groups), electrostatic effects, especially for orienting purposes, can work at a distance [64,65]. A further potential key electrostatic interaction [8\*\*] has now been observed in the two MHC class II complexes [7,8\*\*,11\*], between Lys39 $\alpha$  (in a loop that projects out from the floor of the  $\beta$ -sheet) and Glu56 $\beta$  of the TCR CDR2 $\beta$ .

Another major unresolved issue is how the exceedingly small changes in the TCR/pMHC interface in response to APLs can transmit such different signals via the TCR signalling complex. The slight (or no) increase in complementarity, in BSA or in the number of contacts in agonist versus antagonist complexes are difficult to reconcile with the substantial differences in signalling outcomes that can be generated. Although the trend of increased half-life for agonist versus antagonist TCR/pMHC complexes is so far maintained, exceptions have been found that belie this as a general rule. A telling question that was posed to one of us at a recent international meeting was: if you were given the crystal structures of several agonist and antagonist complexes, could you predict their biological behaviour — can you structurally differentiate the strong from the weak agonist, or the agonist

from the antagonist? The answer is most likely no, since visual inspection of such similar structures cannot resolve the subtle differences in kinetic and thermodynamic properties that lead to such different signalling outcomes.

The TCR itself seems to adapt to small changes in the pMHC ligand by small conformational changes or rearrangements of its central CDR loops. Water molecules themselves may enhance the differences in the interface between agonists and antagonists. The juxtaposition of two membranes, such as in the immunological synapse, many substantially enhance receptor/receptor interactions and exaggerate the extremely small differences in kinetic and thermodynamic parameters that we observe in solution between stable constructs of agonist and antagonist pMHCs.

The future direction of research demands further TCR/pMHC complex structures in order to address these issues and to allow all of the general principles that govern TCR/pMHC recognition to be fully extracted. Perhaps the most important breakthrough of all would be determination of a complete  $\alpha\beta$  TCR signalling complex, including CD4/CD8 and the CD3 $\gamma$ ,  $\delta$ ,  $\epsilon$  and  $\zeta$  chains. Meanwhile, models of the TCR/pMHC/co-receptor (CD4 or CD8) complex can be assembled from the component pieces [16], which include the distal globular domains of CD8/pMHC class I complexes [66,67], the recent low resolution CD4/pMHC class II complex [68] and the CD3 $\epsilon\gamma$  NMR structure [23\*]. Any global changes that could influence TCR signalling events might become apparent from these more complex assemblies. However, the lack of the membrane-anchoring domains in constructs normally used for structure determination will still be a problem until we can routinely crystallise intact membrane proteins. Notwithstanding, substantial advances have certainly been made in the past two years in our understanding of the recognition of MHC class I and now class II by TCRs, as well as structural insights into alloreactivity and graft rejection, and response to APLs. Future studies should also deal with the extent to which bulky ligands — such as substantially bulged peptides [41\*\*], glycopeptides [69,70] or glycolipids in the case of CD1 [71] — can be accommodated in the TCR/pMHC interface.

### Acknowledgements

We thank Robyn Stanfield for substantial help with figures and advice on calculations, Jens Hennecke and Don Wiley for coordinates, Samantha Greasley and Don Wiley for discussions, the Section Editors for comments and Dagmar Klostermeier for critical comments on the manuscript. Our TCR/pMHC research is supported by National Institutes of Health (NIH) grants AI-42266 (to IAW) and CA-58896 (to IAW), a postdoctoral fellowship of the German Academic Exchange Service (to MGR) and the Skaggs Institute for Chemical Biology.

### References and recommended reading

Papers of particular interest, published within the annual period of review, have been highlighted as:

- of special interest
- \*\* of outstanding interest

1. Garcia KC, Degano M, Stanfield RL, Brunmark A, Jackson MR, Peterson PA, Teyton L, Wilson IA: An  $\alpha\beta$  T cell receptor structure at



- 2.5 Å and its orientation in the TCR-MHC complex. *Science* 1996, 274:209-219.
2. Garboczi DN, Ghosh P, Utz U, Fan QR, Biddison WE, Wiley DC: Structure of the complex between human T-cell receptor, viral peptide and HLA-A2. *Nature* 1996, 384:134-141.
  3. Garcia KC, Degano M, Pease LR, Huang M, Peterson PA, Teyton L, Wilson IA: Structural basis of plasticity in T cell receptor recognition of a self peptide-MHC antigen. *Science* 1998, 279:1166-1172.
  4. Degano M, Garcia KC, Apostolopoulos V, Rudolph MG, Teyton L, Wilson IA: A functional hot spot for antigen recognition in a superagonist TCR/MHC complex. *Immunity* 2000, 12:251-261.
- The subtle substitution of an arginine for a lysine in the dEV8 peptide leads to dramatic differences in cytotoxicity, but with few changes in the structure of the two respective complexes. This study indicates that the central region in the interface around peptide residues P4 and P6 represents a 'hotspot', where small substitutions can affect the biological signalling outcome.
5. Ding YH, Smith KJ, Garboczi DN, Utz U, Biddison WE, Wiley DC: Two human T cell receptors bind in a similar diagonal mode to the HLA-A2/Tax peptide complex using different TCR amino acids. *Immunity* 1998, 8:403-411.
  6. Reiser JB, Darnault C, Guimezanes A, Gregoire C, Mosser T, Schmitt Verhulst A-M, Fontecilla-Camps JC, Malissen B, Housset D, Mazza G: Crystal structure of a T cell receptor bound to an allogeneic MHC molecule. *Nat Immunol* 2000, 1:291-297.
- This study formally establishes that allogeneic TCR/pMHC complexes share the same diagonal binding mode as all other MHC class I and class II complexes determined to date. The most interesting feature is the almost complete lack of CDR3 $\alpha$  interactions with the pMHC molecule, leaving a large cavity that is filled by water molecules.
7. Reinherz EL, Tan K, Tang L, Kern P, Liu J, Xiong Y, Hussey RE, Smolyar A, Hare B, Zhang R *et al.*: The crystal structure of a T cell receptor in complex with peptide and MHC class II. *Science* 1999, 286:1913-1921.
  8. Hennecke J, Carfi A, Wiley DC: Structure of a covalently stabilized complex of a human  $\alpha\beta$  T-cell receptor, Influenza HA peptide and MHC class II molecule, HLA-DR1. *EMBO J* 2000, 19:5611-5624.
- In a novel approach, tethering of the peptide to the TCR was used to increase its affinity for the pMHC molecule, thereby facilitating high diffraction-quality crystal growth. This first human TCR/pMHC class II complex highlights the similarities as well as the differences with TCR/pMHC class I complexes.
9. Wilson IA, Stanfield RL: Antibody-antigen interactions: new structures and new conformational changes. *Curr Opin Struct Biol* 1994, 4:857-867.
  10. Ding YH, Baker BM, Garboczi DN, Biddison WE, Wiley DC: Four A6-TCR/peptide/HLA-A2 structures that generate very different T cell signals are nearly identical. *Immunity* 1999, 11:45-56.
  11. Hennecke J, Wiley DC: Structure of a complex of the human  $\alpha\beta$  T cell receptor HA1.7, Influenza HA peptide, and MHC class II molecule, HLA-DR4 (DRA\*0101, DRB\*0401) - insight into TCR cross-restriction and alloreactivity. *J Exp Med* 2001, in press.
- This structure represents the highest resolution TCR/pMHC structure published so far. This alloreactive HLA-DR4 class II MHC complex is very similar to the syngeneic HLA-DR1 structure. However, MHC mutations, which are buried in the peptide-binding groove and not accessible by the TCR, can still indirectly affect TCR recognition by altering the peptide conformation. Many specific water molecules are visible in the TCR/pMHC interface, suggesting a role for water in the recognition process.
12. Allison TJ, Winter CC, Fournie J, Bonneville M, Garboczi DN: Structure of a human  $\gamma\delta$  T-cell antigen receptor. *Nature* 2001, 411:820-824.
- This first determination of a  $\gamma\delta$  TCR crystal structure sheds new light on how  $\gamma\delta$  T cells might serve their various functions including recognition of phosphate antigens and non-classical MHC-like molecules like CD1, T10 and T22.
13. Garcia KC, Teyton L, Wilson IA: Structural basis of T cell recognition. *Annu Rev Immunol* 1999, 17:369-397.
  14. Garcia KC: Molecular interactions between extracellular components of the T-cell receptor signaling complex. *Immunol Rev* 1999, 172:73-85.
  15. Garcia KC, Degano M, Speir JA, Wilson IA: Emerging principles for T cell receptor recognition of antigen in cellular immunity. *Rev Immunogen* 1999, 1:75-90.
  16. Rudd PM, Wormald MR, Stanfield R, Huang M, Mattsson N, Speir JA, DiGennaro JA, Fetrow JS, Dwek RA, Wilson IA: Roles for glycosylation in the cellular immune system. *J Mol Biol* 1999, 293:351-366.
  17. Wang J, Reinherz EL: Structural basis of cell-cell interactions in the immune system. *Curr Opin Struct Biol* 2000, 10:656-661.
  18. Hennecke J, Wiley DC: T cell receptor-MHC interactions up close. *Cell* 2001, 104:1-4.
  19. Rudd PM, Elliott T, Cresswell P, Wilson IA, Dwek RA: Glycosylation and the immune system. *Science* 2001, 291:2370-2376.
  20. Rudolph MG, Luz JG, Wilson IA: Structural and thermodynamic correlates of T cell signaling. *Annu Rev Biophys Biomol Struct* 2002, 31: in press.
  21. Kozono H, White J, Clements J, Marrack P, Kappler J: Production of soluble MHC class II proteins with covalently bound single peptides. *Nature* 1994, 369:151-154.
  22. Wörn A, Plückthun A: Stability engineering of antibody single-chain Fv fragments. *J Mol Biol* 2001, 305:989-1010.
  23. Sun ZJ, Kim KS, Wagner G, Reinherz EL: Mechanisms contributing to T cell receptor signaling and assembly revealed by the solution structure of an ectodomain fragment of the CD3 $\zeta$  heterodimer. *Cell* 2001, 105:913-923.
- First structure of any CD3 component by NMR studies of an engineered covalent dimer of the  $\epsilon$  and  $\gamma$  chains.
24. Poljak RJ, Amzel LM, Avey HP, Becka LN, Goldstein DJ, Humphrey RL: X-ray crystallographic studies of the Fab and Fc fragments of human myeloma immunoglobulins. *Cold Spring Harb Symp Quant Biol* 1972, 36:421-425.
  25. Padlan EA, Segal DM, Spande TF, Davies DR, Rudikoff S, Potter M: Structure at 4.5 Å resolution of a phosphorylcholine-binding Fab. *Nat New Biol* 1973, 245:165-167.
  26. Davies DR, Padlan EA, Segal DM: Three-dimensional structure of immunoglobulins. *Annu Rev Biochem* 1975, 44:639-667.
  27. Li H, Lebedeva MI, Llera AS, Fields BA, Brenner MB, Mariuzza RA: Structure of the V $\delta$  domain of a human  $\gamma\delta$  T-cell antigen receptor. *Nature* 1998, 391:502-506.
  28. Sciammas R, Johnson RM, Sperling AI, Brady W, Linsley PS, Spear PG, Fitch FW, Bluestone JA: Unique antigen recognition by a herpesvirus-specific TCR- $\gamma\delta$  cell. *J Immunol* 1994, 152:5392-5397.
  29. Chien YH, Jores R, Crowley MP: Recognition by  $\gamma\delta$  T cells. *Annu Rev Immunol* 1996, 14:511-532.
  30. Rock EP, Sibbald PR, Davis MM, Chien YH: CDR3 length in antigen-specific immune receptors. *J Exp Med* 1994, 179:323-328.
  31. Wilson IA, Stanfield RL: Unraveling the mysteries of  $\gamma\delta$  T cell recognition. *Nat Immunol* 2001, 2:579-581.
  32. Morita CT, Beckman EM, Bukowski JF, Tanaka Y, Band H, Bloom BR, Golian DE, Brenner MB: Direct presentation of nonpeptide prenyl pyrophosphate antigens to human  $\gamma\delta$  T cells. *Immunity* 1995, 3:495-507.
  33. Belmont C, Espinosa E, Poupot R, Peyrat MA, Guiraud M, Poquet Y, Bonneville M, Fournie JJ: 3-formyl-1-butyl pyrophosphate. A novel mycobacterial metabolite-activating human  $\gamma\delta$  T cells. *J Biol Chem* 1999, 274:32079-32084.
  34. Teng MK, Smolyar A, Tse AG, Liu JH, Liu J, Hussey RE, Nathanson SG, Chang HC, Reinherz EL, Wang JH: Identification of a common docking topology with substantial variation among different TCR-peptide-MHC complexes. *Curr Biol* 1998, 8:409-412.
  35. Shibata K, Imai M, van Bleek GM, Joyce S, Nathanson SG: Vesicular stomatitis virus antigenic octapeptide N52-59 is anchored into the groove of the H-2K $b$  molecule by the side chains of three amino acids and the main-chain atoms of the amino terminus. *Proc Natl Acad Sci USA* 1992, 89:3135-3159.
  36. Bjorkman PJ, Saper MA, Samraoui B, Bennett WS, Strominger JL, Wiley DC: Structure of the human class I histocompatibility antigen, HLA-A2. *Nature* 1987, 329:506-512.
  37. Fremont DH, Matsumura M, Stura EA, Peterson PA, Wilson IA: Crystal structures of two viral peptides in complex with murine MHC class I H-2K $b$ . *Science* 1992, 257:919-927.

38. Zhang W, Young AC, Imarai M, Nathenson SG, Sacchettini JC: Crystal structure of the major histocompatibility complex class I H-2K<sup>b</sup> molecule containing a single viral peptide: Implications for peptide binding and T-cell receptor recognition. *Proc Natl Acad Sci USA* 1992, 89:8403-8407.
39. Silver ML, Guo HC, Strominger JL, Wiley DC: Atomic structure of a human MHC molecule presenting an influenza virus peptide. *Nature* 1992, 360:367-369.
40. Stern LJ, Wiley DC: Antigenic peptide binding by class I and class II histocompatibility proteins. *Structure* 1994, 2:245-251.
41. Speir JA, Stevens J, Joly E, Butcher GW, Wilson IA: Two different, highly exposed, bulged structures for an unusually long peptide bound to rat MHC class I RT1-A\*. *Immunity* 2001, 14:81-92.
- The first structure of a long peptide (13-mer) in complex with a rat class I MHC molecule shows two well-ordered conformations that contain extreme bulges for the central residues of the peptide. This extensive bulging and mass that needs to be accommodated in the TCR/pMHC interface has profound structural implications on how TCRs must be able to adapt for the recognition of such complexes.
42. Young AC, Zhang W, Sacchettini JC, Nathenson SG: The three-dimensional structure of H-2D<sup>b</sup> at 2.4 Å resolution: Implications for antigen-determinant selection. *Cell* 1994, 76:39-50.
43. Speir JA, Garcia KC, Brunmark A, Degano M, Peterson PA, Teyton L, Wilson IA: Structural basis of 2C TCR allorecognition of H-2L<sup>d</sup> peptide complexes. *Immunity* 1998, 8:553-562.
44. Matsui K, Boniface JJ, Reay PA, Schild H, Fazekas de St Groth B, Davis MM: Low affinity interaction of peptide-MHC complexes with T cell receptors. *Science* 1991, 254:1788-1791.
45. Baker BM, Gagnon SJ, Biddison WE, Wiley DC: Conversion of a T cell antagonist into an agonist by repairing a defect in the TCR/peptide/MHC interface: implications for TCR signaling. *Immunity* 2000, 13:475-484.
- Using non-natural amino acids, the systematic filling of a cavity – created by a peptide residue mutation in the TCR/pMHC interface – leads to a stepwise increase in both affinity and peptide-presentation ability.
46. Garcia KC, Scott CA, Brunmark A, Carbone FR, Peterson PA, Wilson IA, Teyton L: CD8 enhances formation of stable T-cell receptor/MHC class I molecule complexes. *Nature* 1996, 384:577-581.
47. Baker BM, Wiley DC:  $\alpha\beta$  T cell receptor ligand-specific oligomerization revisited. *Immunity* 2001, 14:681-692.
48. Reich Z, Boniface JJ, Lyons DS, Borochov N, Wachtel EJ, Davis MM: Ligand-specific oligomerization of T-cell receptor molecules. *Nature* 1997, 387:617-620.
49. Krummel M, Wulfig C, Sumen C, Davis MM: Thirty-six views of T-cell recognition. *Philos Trans R Soc Lond B Biol Sci* 2000, 355:1071-1076.
50. Manning TC, Kranz DM: Binding energetics of T-cell receptors: correlation with immunological consequences. *Immunol Today* 1999, 20:417-422.
51. Braden BC, Goldman ER, Mariuzza RA, Poljak RJ: Anatomy of an antibody molecule: structure, kinetics, thermodynamics and mutational studies of the antilysozyme antibody D1.3. *Immunol Rev* 1998, 163:45-57.
52. Al-Lazikani B, Lesk AM, Chothia C: Canonical structures for the hypervariable regions of T cell  $\alpha\beta$  receptors. *J Mol Biol* 2000, 295:979-995.
- A classification of the CDR loop conformations in the available TCR and TCR/pMHC structures. The key residues that determine each canonical structure are identified.
53. Chothia C, Lesk AM: Canonical structures for the hypervariable regions of immunoglobulins. *J Mol Biol* 1987, 196:901-917.
54. Chothia C, Lesk AM, Tramontano A, Levitt M, Smith-Gill SJ, Air G, Sheriff S, Padlan EA, Davies D, Tulip WR: Conformations of immunoglobulin hypervariable regions. *Nature* 1989, 342:877-883.
55. Bjorkman PJ, Davis MM: Model for the interaction of T-cell receptors with peptide/MHC complexes. *Cold Spring Harb Symp Quant Biol* 1989, 54:365-373.
56. Al-Lazikani B, Lesk AM, Chothia C: Standard conformations for the canonical structures of immunoglobulins. *J Mol Biol* 1997, 273:927-948.
57. Davis M, Boniface J, Reich Z, Lyons D, Hampl J, Arden B, Chien Y: Ligand recognition by  $\alpha\beta$  T cell receptors. *Annu Rev Immunol* 1998, 16:523-544.
58. Willcox BE, Gao GF, Wyer JR, Ladbury JE, Bell JI, Jakobsen BK, van der Merwe PA: TCR binding to peptide-MHC stabilizes a flexible recognition interface. *Immunity* 1999, 10:357-365.
59. Boniface JJ, Reich Z, Lyons DS, Davis MM: Thermodynamics of T cell receptor binding to peptide-MHC: evidence for a general mechanism of molecular scanning. *Proc Natl Acad Sci USA* 1999, 96:11446-11451.
60. Bhat TN, Bentley GA, Boulton G, Greene MI, Tello D, Dall'Acqua W, Souchon H, Schwarz FP, Mariuzza RA, Poljak RJ: Bound water molecules and conformational stabilization help mediate an antigen-antibody association. *Proc Natl Acad Sci USA* 1994, 91:1089-1093.
61. Rudolph MG, Speir JA, Brunmark A, Mattsson N, Jackson MR, Peterson PA, Teyton L, Wilson IA: The crystal structures of K<sup>b</sup>m1 and K<sup>b</sup>m8 reveal that subtle changes in the peptide environment impact thermostability and alloreactivity. *Immunity* 2001, 14:231-242.
- Mouse natural mutant-peptide/MHC complexes were determined to the highest resolution (1.7 Å) so far and identified many water molecules around the peptide binding site. The implication of water molecules in T-cell recognition and the structural basis for alloreactivity are discussed.
62. Porcelli SA, Segelke BW, Sugita M, Wilson IA, Brenner MB: The CD1 family of lipid antigen-presenting molecules. *Immunol Today* 1998, 19:362-368.
63. Wilson IA: Class-conscious TCR? *Science* 1999, 286:1867-1868.
64. Schreiber G, Frisch C, Fersht AR: The role of Glu73 of barnase in catalysis and the binding of barstar. *J Mol Biol* 1997, 270:111-122.
65. McCoy AJ, Chandana-Epa V, Colman PM: Electrostatic complementarity at protein/protein interfaces. *J Mol Biol* 1997, 268:570-584.
66. Gao GF, Tormo J, Gerth UC, Wyer JR, McMichael AJ, Stuart DI, Bell JI, Jones EY, Jakobsen BK: Crystal structure of the complex between human CD8 $\alpha\alpha$  and HLA-A2. *Nature* 1997, 387:630-634.
67. Kern PS, Teng MK, Smolyar A, Liu JH, Liu J, Hussey RE, Spoerl R, Chang HC, Reinherz EL, Wang JH: Structural basis of CD8 coreceptor function revealed by crystallographic analysis of a murine CD8 $\alpha\alpha$  ectodomain fragment in complex with H-2K<sup>b</sup>. *Immunity* 1998, 9:519-530.
68. Wang J, Meijers R, Xiong Y, Liu J, Sakihama T, Zhang R, Joachimiak A, Reinherz EL: Crystal structure of the human CD4 N-terminal two domain fragment complexed to a class II MHC molecule. *Proc Natl Acad Sci USA* 2001, 98:10799-10804.
69. Speir JA, Abdel-Motal UM, Jondal M, Wilson IA: Crystal structure of an MHC class I presented glycopeptide that generates carbohydrate-specific CTL. *Immunity* 1999, 10:51-61.
70. Glithero A, Tormo J, Haurum JS, Arsequell G, Valencia G, Edwards J, Springer S, Townsend A, Pao YL, Wormald M et al.: Crystal structures of two H-2D<sup>b</sup>/glycopeptide complexes suggest a molecular basis for CTL cross-reactivity. *Immunity* 1999, 10:63-74.
71. Moody DB, Besra GS, Wilson IA, Porcelli SA: The molecular basis of CD1-mediated presentation of lipid antigens. *Immunol Rev* 1999, 172:285-296.
72. Berman HM, Westbrook J, Feng Z, Gilliland G, Bhat TN, Weissig H, Shindyalov IN, Bourne PE: The Protein Data Bank. *Nucleic Acids Res* 2000, 28:235-242.
73. Connolly ML: The molecular surface package. *J Mol Graph* 1993, 11:139-141.
74. McDonald IK, Thornton JM: Satisfying hydrogen bonding potential in proteins. *J Mol Biol* 1994, 238:777-793.
75. Sheriff S, Hendrickson WA, Smith JL: Structure of myohemerythrin in the azidomet state at 1.7/1.3 Å resolution. *J Mol Biol* 1987, 197:273-296.